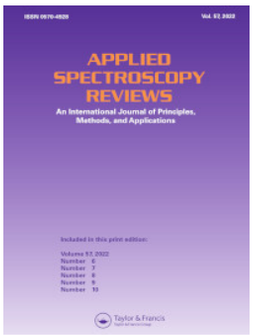

Taylor & Francis
Taylor & Francis Group

Applied Spectroscopy Reviews

ISSN: (Print) (Online) Journal homepage: www.tandfonline.com/journals/laps20

Techniques for measuring indoor radicals and radical precursors

Elena Gómez Alvarez, Nicola Carslaw, Sébastien Dusanter, Pete Edwards, Viktor Gábor Mihucz, Dwayne Heard, Jörg Kleffmann, Sascha Nehr, Coralie Schoemacker & Dean Venables

To cite this article: Elena Gómez Alvarez, Nicola Carslaw, Sébastien Dusanter, Pete Edwards, Viktor Gábor Mihucz, Dwayne Heard, Jörg Kleffmann, Sascha Nehr, Coralie Schoemacker & Dean Venables (2022) Techniques for measuring indoor radicals and radical precursors, Applied Spectroscopy Reviews, 57:7, 580-624, DOI: 10.1080/05704928.2022.2087666

To link to this article: https://doi.org/10.1080/05704928.2022.2087666

© 2022 The Author(s). Published with license by Taylor and Francis Group, LLC

Published online: 25 Jun 2022.

Submit your article to this journal

Article views: 2147

View related articles

View Crossmark data

Citing articles: 3 View citing articles

Full Terms & Conditions of access and use can be found at
https://www.tandfonline.com/action/journalInformation?journalCode=laps20

APPLIED SPECTROSCOPY REVIEWS
2022, VOL. 57, NO. 7, 580–624
https://doi.org/10.1080/05704928.2022.2087666

Taylor & Francis
Taylor & Francis Group

Techniques for measuring indoor radicals and radical precursors

Elena Gómez Alvarez[a], Nicola Carslaw[b], Sébastien Dusanter[c], Pete Edwards[d], Viktor Gábor Mihucz[e], Dwayne Heard[f], Jörg Kleffmann[g], Sascha Nehr[h], Coralie Schoemacker[i], and Dean Venables[j]

[a]Department of Agronomy, University of Córdoba, Campus de Rabanales, Córdoba, Spain; [b]Department of Environment and Geography, University of York, York, UK; [c]Centre for Energy and Environment, IMT Nord Europe, University of Lille, Institut Mines-Télécom, Lille, France; [d]Wolfson Atmospheric Chemistry Laboratory, Department of Chemistry, University of York, York, UK; [e]Department of Analytical Chemistry, Institute of Chemistry, ELTE- Eötvös Loránd University, Budapest, Hungary; [f]School of Chemistry, University of Leeds, Leeds, UK; [g]Physical and Theoretical Chemistry, University of Wuppertal, Wuppertal, Germany; [h]CBS International Business School, Brühl, Germany; [i]Bât. C11, Cité Scientifique, CNRS-Université de Lille, Villeneuve d'Ascq, France; [j]School of Chemistry and Environmental Research Institute, University College Cork, Cork, Ireland

ABSTRACT

Radicals and their precursors play a central role in the chemical transformations occurring in indoor air and on indoor surfaces. Such species include OH, HO_2, peroxy radicals, nitrous acid, reactive chlorine species, NO_3, N_2O_5, Criegee intermediates, and glyoxal and methylglyoxal. Recent advances on instrumental analysis and modeling studies have demonstrated the need for a wider range of measurements of radical species and their precursors in indoor air. This work reviews measurement techniques and provides considerations for indoor measurements of several radicals and their precursors. Techniques to determine the actinic flux are also presented owing to the relevance of photolytically-initiated processes indoors. This review is also intended to provide pointers for those wanting to learn more about measurements of radicals indoors.

KEYWORDS

Criegee; peroxy; HONO; FAGE; CIMS; Laser-induced fluorescence

1. Introduction

A small group of highly reactive species, often radicals and their precursors, play a central role in the chemical transformations occurring in indoor air and on indoor surfaces. Reactions involving these species affect indoor air quality through the loss of reactants and the formation of new chemical species whose toxicity could differ substantially from their precursors. Since reaction products are often of lower volatility than their parent compounds, these reactions can also lead to the growth or formation of particulate matter.

Measuring the concentrations of highly reactive species is challenging for several reasons:

CONTACT Elena Gómez Alvarez qa2goalm@uco.es University of Cordoba, Córdoba, Spain; Dean Venables d.venables@ucc.ie School of Chemistry and Environmental Research Institute, University College Cork, Cork, Ireland

© 2022 The Author(s). Published with license by Taylor and Francis Group, LLC
This is an Open Access article distributed under the terms of the Creative Commons Attribution-NonCommercial-NoDerivatives License (http://creativecommons.org/licenses/by-nc-nd/4.0/), which permits non-commercial re-use, distribution, and reproduction in any medium, provided the original work is properly cited, and is not altered, transformed, or built upon in any way.

- mixing ratios in indoor air are often extremely low
- inlet losses can be problematic. Instrument residence times and material selection are therefore important considerations
- pre-concentration is not generally viable as a measurement strategy as it is with stable organic compounds
- instrument calibration and validation studies are complicated by the absence of commercially available reference materials

Moreover, practical issues like instrument size, noise, and hazards associated with lasers and electrical cables need to be considered in occupied indoor spaces.

Based on the assumption that indoor radical concentrations were much lower than outdoors, the study of reactive indoor chemistry was initially restricted to ozone chemistry. However, first modeling and then experimental studies began to question this assumption and indicated that concentrations of radicals can be on the same order of magnitude as that observed outdoors, or even larger for chlorine radicals under circumstances such as cleaning. Indoor radicals can derive from sources indoors (such as cleaning or air-freshener use) or through infiltration of radical precursors (VOC, O_3 and NO_X) from outside air.

Transmission of UV and visible light into buildings plays a fundamental role in the generation of radicals. Outdoors, oxidation is driven by photochemistry, often initiated by sunlight at wavelengths shorter than 320 nm. Such high energy photons are not generally available indoors and the oxidizing capacity can be dominated by infiltration of reactant species from outdoor air and by non-photochemical reactions (also known as "dark chemistry") [1]. This results in different oxidizing atmospheres indoors and outdoors.

Recent studies suggest that photolysis of molecules that absorb light at wavelengths longer than 320 nm, such as nitrous acid (HONO) and formaldehyde (HCHO), may lead to higher indoor hydroxyl radical (OH) concentrations than previously expected. Gomez Alvarez et al.[2] provided the first direct experimental confirmation that the indoor levels of OH radicals are comparable to outdoor concentrations. Particularly noteworthy are activities that lead to high indoor concentrations of these species, such as of HONO following combustion[3]. HONO photolysis can compensate for the missing OH formation by ozone photolysis, which is normally the dominant source of OH radicals outdoors.

Indoor cleaning can also lead to radical production. Carslaw et al.[4] reported measurements of OH and hydroperoxy (HO_2) radicals made by laser-induced fluorescence spectroscopy in a computer classroom, (i) in the absence of indoor activities, (ii) during desk cleaning with a limonene-containing cleaner and (iii) during operation of a commercially available "air cleaning" device. In the unmanipulated environment, the one-minute averaged OH concentration remained close to or below the limit of detection (6.5×10^5 molecules cm^{-3}), while HO_2 was 1.3×10^7 molecules cm^{-3}. These concentrations increased to $\sim 4 \times 10^6$ and 4×10^8 molecules cm^{-3}, respectively during desk cleaning. During operation of the air cleaning device, OH and HO_2 concentrations reached $\sim 2 \times 10^7$ and $\sim 6 \times 10^8$ molecules cm^{-3}, respectively.

Owing to the presence of O_3 and nitrogen dioxide (NO_2) indoors and the relatively low light levels, it might be expected that the nitrate radical (NO_3) could attain

significant indoor concentrations. Arata et al.[5] conducted direct indoor measurements of the nitrate radical (NO_3) and dinitrogen pentoxide (N_2O_5) produced following combustion cooking emissions in a residential kitchen. They concluded that indoor combustion suppresses nitrate radical chemistry when O_3 concentrations are low, but at moderate O_3 levels (~40 ppbv), measured NO_3 concentrations reached 3–4 pptv. A box model showed that moderate O_3 levels led to a nitrate radical production rate of 7 ppbv h^{-1}.

It has also recently been shown that cleaning activities using chlorine-based cleaners including use of bleach can lead to the formation of numerous reactive chlorine (Cl) species, many of which are photo-labile and could generate atomic Cl indoors. Wong et al.[6] measured concentrations of chlorinated gases and aerosol components using online chemical ionization and aerosol mass spectrometers after an indoor floor was repeatedly washed with a commercial bleach solution. Gaseous chlorine (Cl_2) at mixing ratios of tens of ppbv and hypochlorous acid (HOCl) at mixing ratios of hundreds of ppbv were observed after floor washing. Nitryl chloride ($ClNO_2$), dichlorine monoxide (Cl_2O), and chloramines ($NHCl_2$, NCl_3) were also formed under these conditions. Photochemical box models indicated that OH, Cl, and chlorine monoxide (ClO) gas-phase radical concentrations could be greatly enhanced ($>10^6$ and 10^5 molecules cm^{-3} for OH and Cl, respectively) in such bleach cleaning conditions, depending on the amount of indoor illumination[6]. Dark chemistry during bleach cleaning and use of surface disinfectants also affects indoor air quality by enhancing oxidation of organics and production of secondary organic aerosols indoors [7,8].

Gandolfo et al.[9] provided direct measurements and modeling of the actinic flux and photolysis frequencies of species relevant for indoor atmospheres (HONO, NO_2 and NO_3) during summer and winter periods. Zhou et al.[10] measured wavelength-resolved ultraviolet (UV) irradiance in multiple indoor environments and quantified the effects of variables such as light source, solar angles, cloud cover, window type, and electric light color temperature on indoor photon fluxes. They reported mathematical relationships that predict indoor solar UV irradiance as a function of solar zenith angle, incident angle of sunlight on windows, and distance from windows and surfaces for direct and diffuse sunlight. Using these relationships, they predict elevated indoor steady-state OH concentrations ($0.80–7.4 \times 10^6$ molecules cm^{-3}) under illumination by direct and diffuse sunlight and fluorescent tubes near windows or light sources. In a later study, Zhou et al. [11] made intensive measurements of wavelength-resolved spectral irradiance in a test house during the HOMEChem campaign and reported diurnal profiles and two-dimensional spatial distribution of photolysis rates (J) of several important indoor photolabile gases. Their results showed that sunlight transmitted through windows, which was the dominant source of ultraviolet (UV) light in the test house, led to clear diurnal cycles and large time- and location-dependent variations in local gas-phase photochemical activity. Compared to diffuse sunlight, local J values of several key indoor gases under direct solar illumination were 1.8–7.4 times larger and strongly dependent on time, solar zenith angle, and incident angle of sunlight relative to the window. Photolysis rates were highly spatially heterogeneous and fast photochemical reactions in the gas phase were generally confined to within tens of centimeters of the area exposed to direct sunlight. Opening windows increased UV photon fluxes by a

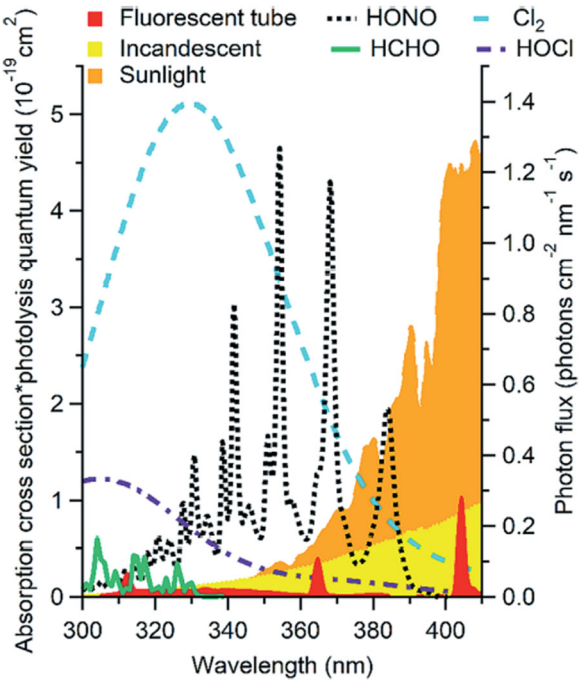

Figure 1. Photon flux of common indoor light sources (right axis, arbitrary scale) shown with the product of absorption cross section and photolysis quantum yield of likely indoor oxidants (left axis). Actinic fluxes of the indoor lamps were measured at a short distance. Reproduced from Young et al.[1], with permission from the Royal Society of Chemistry.

factor of 3 and increased predicted local hydroxyl radical (OH) concentrations in the sunlit region by a factor of 4.5, leading to a concentration of 3.2×10^7 molecules cm^{-3} as a result of higher J values and an increased contribution from O_3 photolysis. Figure 1 displays photon fluxes of indoor light sources and the product of absorption cross section and photolysis quantum yield of likely indoor oxidants.

The above overview of recent measurements and modeling studies demonstrates the need for a wider range of measurements of radical species and their precursors in indoor air. This paper therefore focuses on reviewing measurement techniques and provides considerations for indoor measurements of OH, HO_2, and peroxy radicals, OH reactivity, the OH radical precursor, nitrous acid, reactive chlorine species, NO_3 and its atmospheric reservoir N_2O_5, Criegee intermediates, and the bicarbonyl species glyoxal and methylglyoxal indoors. Techniques to measure the actinic flux are also presented owing to the relevance of photolytically-initiated processes indoors. The inorganic species NO, NO_2, and O_3 were omitted as they are routinely measured relatively straightforwardly.

This review of indoor radicals and radical precursor measurement techniques is intended to provide some pointers for those wanting to learn more about radical concentrations indoors. It is based on recent innovations for radical measurements and connected species/parameters. It is not an exhaustive review of all possible techniques. For instance, Matrix Isolation Electron Spin Resonance (MIESR) has been superseded

Table 1. Concentration range of the radicals in the atmosphere. Note that for CH_3O_2 this represents a model estimate only.

Radical(s)	**Atmospheric concentration** (molecules cm^{-3})
OH	10^5-10^7
HO_2	10^6-10^9
CH_3O_2	10^6-10^8
sum RO_2	10^6-10^9

by other methods and long physical path methods like multi-pass Differential Optical Absorption Spectroscopy (DOAS) are normally too bulky for indoor measurements.

2. Measurements techniques of radicals and radical precursors indoors

2.1. Hydroxyl and hydroperoxy radicals

Oxidation of volatile organic compounds produces radical species indoors. These gas-phase oxidation reactions transform primary VOC emissions into secondary species (including into harmful pollutants), and involve the OH and HO_2 radicals, collectively known as HO_x. There is a need to better understand the chemical transformations of multiple VOC species that are present indoors and the potential impact of their oxidation on indoor air quality and human health. Doing so requires the measurement of radical concentrations and the secondary species which derive from them in real-life environments. Such measurements will permit the further development of chemical mechanisms for models and to gain further insight.

Owing to the short-lived nature of radical species (for example, <1 second for OH), their local concentrations are controlled by the rate at which they are chemically formed and removed, and not by transport processes. As a result, comparing measured and modeled concentration profiles of oxidants such as OH radicals is an ideal test of how well we understand the details of these chemical transformations. Another parameter linked to the OH radical is the pseudo-first-order rate coefficient at which OH is removed by its sinks, known as the OH reactivity. This parameter is representative of all the chemical losses of OH. The OH reactivity can be measured in ambient air by coupling a reactor in which OH is generated to instruments able to quantify OH or OH reactivity.

Peroxy radicals, which comprise both HO_2 and organic RO_2 (where R is an organic group), are key intermediate species in the oxidation process. These radicals facilitate fast chemical cycles that reform OH and, in the presence of NO, lead to the formation of NO_2 which can photolyze to generate ozone. The central role of RO_2 and their short lifetimes make measurements of their concentrations useful for comparison with model predictions. However, the measurement of these radicals is an experimental challenge owing to their high reactivity, short lifetimes, and low concentrations. Table 1 summarizes typical concentrations of radicals in the atmosphere, including indoor environments.

A range of instruments have been developed to measure HO_x radicals in the atmosphere using optical and mass spectrometric techniques [12–14].

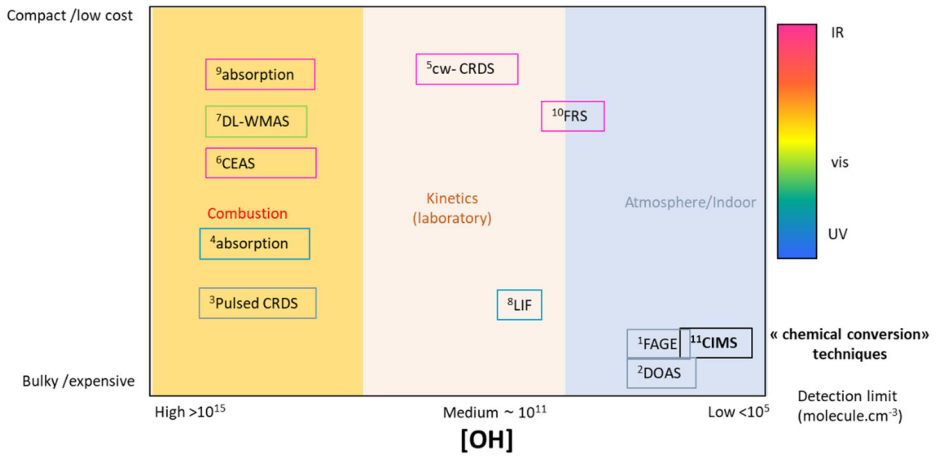

Figure 2. Techniques currently used to quantify OH in reactive systems: FAGE[1] [15], DOAS[2][16], Cavity Ringdown Spectroscopy (CRDS)[3] [17], Diode-laser-based UV absorption[4] [18], cw-CRDS[5] [19,20], Cavity-Enhanced Absorption Spectroscopy (CEAS)[6] [21], Diode-Laser wavelength Wavelength Modulation Absorption Spectroscopy (DL-WMAS)[7] [22], Laser-Induced Fluorescence (LIF) (FAGE)[8] [23], diode laser absorption[9] [24], Faraday Rotation Spectroscopy (FRS)[10] [25], CIMS[11] [26].

2.1.1. OH quantification

The techniques currently used for OH are Fluorescence Assay by Gas Expansion (FAGE), Chemical Ionization Mass Spectrometry (CIMS) and Differential Optical Absorption Spectroscopy (DOAS), although DOAS is now retired from field use and is only used at one outdoor atmospheric simulation chamber (SAPHIR at Jülich). Figure 2 shows a range of methods for quantifying OH across a range of concentrations. Techniques based on the measurement of a tracer have been used indoors and in atmospheric simulation chambers (e.g., HIRAC, EUPHORE and SAPHIR).

2.1.2. FAGE technique principle

The FAGE (Fluorescence Assay by Gas Expansion) technique is based on detection of Laser Induced Fluorescence (LIF) detection of OH after excitation at 308 nm. The sample is at low pressure, after a gas expansion formed by sampling the atmosphere through a small pinhole. As of 2021, the FAGE technique is the approach most commonly used in field campaigns. Eleven groups in the world have developed instruments: University of Leeds[27], Max Planck Institute in Mainz[28], Forschungszentrum Jülich[29], EUPHORE chamber in Valencia (http://www.ceam.es/wwweuphore/), Pennsylvania State University[15], University of Indiana at Bloomington [30], University of Lille [31], Peking University in collaboration with the Forschungszentrum Jülich[32], and Hefei[33].

Recently, a modification to the FAGE sampling methodology has been made which uses an inlet pre-injector (IPI) to add a chemical scavenger to remove any ambient OH prior to sampling by the pinhole and entering the fluorescence cell [28,34–36]. A measurement using the IPI is known as OH-Chem, and is different to OH-Wave, which uses wavelength modulation of the laser to measure the background signal. Through the use of the IPI, any remaining LIF signal from OH must have originated from artificially generated OH from an interference present within the fluorescence cell itself, and

enables removal of this interference signal. OH-Chem and OH-Wave are similar for most conditions.

2.1.3. CIMS instrument principle

OH can be converted to H_2SO_4 by titration with SO_2, with subsequent detection as H_2SO_4 using CIMS and ionization based on its reaction with NO_3^- ions. As the concentration of OH is low, isotopically labeled $^{34}SO_2$ is used to reduce interferences from naturally present H_2SO_4. At present, three groups use CIMS instruments for the quantification of OH in the field[37–39]. Isotopically labeled $^{34}SO_2$ is very expensive and shortages of it have been known. However, it increases the precision of the measurement as background levels of H_2SO_4 can be significant.

2.1.4. DOAS instrument principle

DOAS measurement of OH has been developed in the UV (at 308 nm), where the absorption cross sections for OH are large and well known[16]. DOAS has the advantage of providing an absolute OH concentration but requires a long absorption path (several km) to reach a sensitivity high enough for atmospheric applications[40]. The only current operational instrument for OH measurements is permanently installed in the large SAPHIR chamber in Jülich. The SAPHIR instrument has a multipass cell with a base length of 20 m and a total path length of 2.24 km, giving a limit of detection (LoD) of 7.3×10^5 molecules cm^{-3} for 200 s integration time [41].

2.1.5. OH reactivity

The measurement of OH reactivity has been developed over the last 2 decades for atmospheric applications. This parameter corresponds to the sum of all losses of OH and complements other measurements characterizing the oxidation processes linked to OH. It measures the first order rate coefficient of the OH loss in a single measurement. When compared with model calculations it allows evaluation of whether all the sinks of OH are accurately captured in the chemical mechanism. For this, the directly measured OH destruction rate is compared against the destruction rate inferred from other field measurements. When coupled to the measured OH concentration and to measurements characterizing the major OH-producing pathways (HO_2 + NO, HONO-photolysis and O_3-photolysis), it also allows to analyze OH budgets exclusively on experimental data. The overall OH production rate is given by OH-recycling via the HO_2 + NO reaction plus the primary production rates mainly resulting from photolysis of HONO and O_3. The overall OH destruction rate is given by the product of total OH reactivity and the OH concentration.

Three techniques have been developed which generate artificial OH in a reactor containing ambient air and measure its decay either directly or indirectly:

1. two are based on OH detection techniques already used for the atmospheric measurement of OH concentrations (FAGE based on the LIF technique, and CIMS) and coupled to different types of reactors: Flow Tube (FT) or Laser

Photolysis reactor (LP) coupled to a FAGE instrument. These two correspond to the following techniques: FT-LIF, FT-CIMS, LP-LIF

2. one based on the measurement of a tracer reacting with OH (Comparative Reactivity Method, CRM)

The FT-LIF method is based on the continuous generation of OH radicals in a flow tube by photolysis of H_2O vapor by a mercury lamp placed in a moving injector, allowing measurement of OH at different reaction times corresponding to different positions of the injector, with the detection of OH by FAGE[42]. Corrections are needed for the recycling of HO_2 (generated simultaneously with OH) into OH in the presence of NO in ambient air.

The LP-LIF is based on detection of OH by FAGE, similarly to FT-LIF, but OH is generated in a reactor by pulsed photolysis of ozone at 266 nm in the presence of water vapor[43]. In contrast to FT-LIF, this approach has the advantage of generating only OH, limiting recycling of ambient HO_2 to OH only to high NO conditions. Another advantage is that the OH is directly monitored as a function of time, and conversion from a physical parameter (distance) into time is not required.

The FT-CIMS uses the same OH generation method to FT-LIF but OH is converted first into H_2SO_4 and detected by CIMS. The measurement is made at one reaction time by alternatively injecting sulfur dioxide in the reactor at the entrance or at a position corresponding to a detection time of about 75 ms[44]. Corrections are also needed for recycling of ambient HO_2 into OH with NO.

The CRM technique does not directly measure OH but rather measures a tracer reacting with it. It is based on the competition between the reactions of OH with all species present in ambient air and with the tracer molecule added to the flow. OH is produced in a reactor by continuous photolysis of H_2O vapor using a mercury lamp and the tracer is quantified by a suitable detector at the exit of the reactor. Pyrrole (C_4H_5N) is currently used as the tracer.

The methods used to measure OH reactivity, together with their performance details, are summarized in Table 2. The data in Table 2 is from two intercomparison campaigns of OH reactivity that took place in the atmospheric simulation chamber SAPHIR in Forschungszentrum Jülich in October 2015 and April 2016[45]. The intercomparison gathered all the instruments then used for the determination of OH radicals.

The column corresponding to OH concentration in Table 2 is what is generated inside the instrument to perform the OH reactivity measurement. For example, in the LP-LIF method, OH is generated by photolysis of ozone at 266 nm followed by the reaction of $O(^1D)$ with H_2O vapor at a certain laser power. The O_3 and H_2O concentrations vary between instruments and therefore affect the initial OH generated (column [OH] in Table 2).

2.1.6. HO_2 quantification

HO_2 is most frequently quantified by indirect detection based on converting HO_2 to OH and subsequent detection as OH using FAGE or CIMS instruments. However, titration by NO can also convert some RO_2 to HO_2. In FAGE instruments, modulation of NO is used to selectively detect HO_2[32,55–57]. With PeRCIMS instruments (Peroxy

Table 2. Performance characteristics of instruments used to measure OH reactivity from two intercomparison campaigns. [45]

Instrument	Technique	Time res. [s]	1σ LOD[a] [s^{-1}]	1σ accuracy[a] (k_{OH})	Flow rate [L min^{-1}]	[OH] [10^{10} molecules cm^{-3}]	Inlet res. Time [s]	Inlet line	Reference
MDOUAI [b]	CRM[c]	600	1	18%	0.37 [d]	72 [e,f]	5	1/4″ PFA	[46]
LSCE [b]	CRM[c]	600	1	35%	0.23 [d]	78 [e,f]	6	1/4″ PFA	[47]
MPI [b,g]	CRM[c]	900	1.6[b] 1.3[g]	37%	0.38	75 [e,f]	6	1/4″ PFA (heated)[b] 1/2″ PFA (heated)[g]	[48]
PSU [b]	FT-LIF[i]	30	0.5[i]	23% (<2 s^{-1}) 8% (10—100 s^{-1}) 7% (>100 s^{-1})	100	0.5 [e]	1	1″ PFA	[42,49]
Lille [b]	LP-LIF[h]	30—60	0.4	8%	9.5	0.6 [k]	4	1/2″ PFA	[50]
Leeds [b]	LP-LIF[h]	100	0.4—1.0	6%	16	3 [k]	2.5	1/2″ PFA	[51]
FZJ M [b]	LP-LIF[h]	40—160	0.2	10%	15	0.7 [k]	0.5	10 mm steel (Silconert coating)	[52,53]
FZJ S [b,g]	LP-LIF[h]	60	0.1	10%	20	0.8 [k]	0.5	10 mm steel (Silconert coating)	[52]
DWD [g]	FT-CIMS[l]	60—300	0.5	1 s^{-1} (<30 s^{-1}) 2 s^{-1} (30—40 s^{-1})	2280 [m]	0.01 [e]	No additional inlet line		[54]

[a] Limit of detection/accuracy as stated by the operator. [b] October 2015. [c] Comparative reactivity measurement. [d] Faster flow of 1 L min^{-1} in inlet line. [e] Produced continuously by water photolysis by a PenRay lamp. [f] Derived from the difference in the C1 and C2 measurement (C1 and C2 are specific to the CRM instruments and represent two different conditions within the instrument depending on whether ambient air is introduced or not). [g] April 2016. [h] Laser flash photolysis and laser induced fluorescence. [i] Flow-tube and laser-induced fluorescence. [j] Limit of detection without the dilution, which amplifies this number by a factor of 5. [k] Peak value produced by flash ozone photolysis at 266 nm. [l] Flow tube and chemical ionization mass spectrometry. [m] Sampling rate from the chamber.

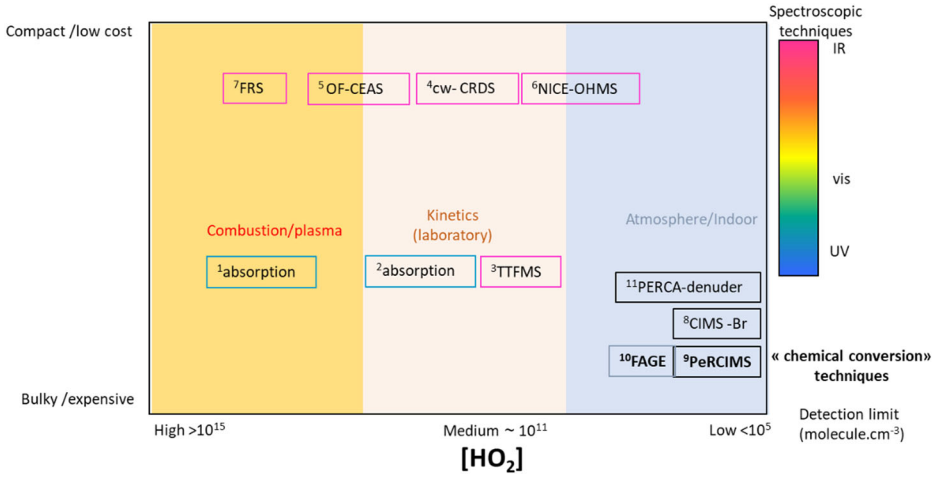

Figure 3. Techniques currently used to quantify HO_2 in reactive systems: [1] Absorption Spectroscopy[64] [2]Flash Photolysis UV Absorption[65] [3]Near-Infrared Wavelength Modulation Spectroscopy&UV Absorption Spectroscopy[66] [4]cw-CRDS[67] [5]Optical Feedback Cavity Enhanced Absorption Spectroscopy[68] [6]Noise-Inmune Cavity Enhanced Optical Heterodyne Detection[69] [7]Mid-Infrared Faraday Rotation Spectrometry[70] [8]Bromide Chemical Ionization Mass Spectrometry[63] [9]Peroxy Radical Chemical Ionization Mass Spectrometry[59] [10]FAGE[56] [11]PERCA-denuder[61].

Radical Chemical Ionization Mass Spectrometry), depending on the concentration of O_2, NO and SO_2 and diluting the air sampled with either O_2 or N_2, it is possible to speciate measurements of either RO_2 or HO_2 [14,58–60] but only if CH_3O_2 is the major contribution to total RO_2. A modified PERCA (peroxy radical chemical amplification) instrument dedicated to the sum of RO_2 measurement, using detection of NO_2 by LIF, has been tested to selectively quantify HO_2 using a denuder with heterogeneous losses higher for HO_2 than for RO_2[61]. Bromide has recently been shown to be a useful reagent ion for CIMS detection of HO_2 with high selectivity and at concentrations relevant to many ambient conditions [62,63]. Approaches to measure HO_2 are shown in Figure 3.

2.2. Peroxy (RO_2) radicals

Quantification of RO_2 radicals is more complex than for OH and HO_2, because the peroxy radicals comprise a family of radicals and not an individual species. As a result, most techniques only allow measurement of the sum of all RO_2 or of a sub-group of RO_2. Efforts have been made to selectively measure CH_3O_2, the main RO_2 radical in the atmosphere. Selective quantification of CH_3O_2 is possible by titrating with NO and detection as CH_3O with laser-induced fluorescence. This approach has been demonstrated in the HIRAC (Highly Instrumented Reactor for Atmospheric Chemistry) chamber[71], where an intercomparison was also performed with the less sensitive cavity-ring down method[72].

Other techniques for unspeciated RO_2 measurements are based on similar detection methods to those used for HO_2, after converting RO_2 into HO_2:

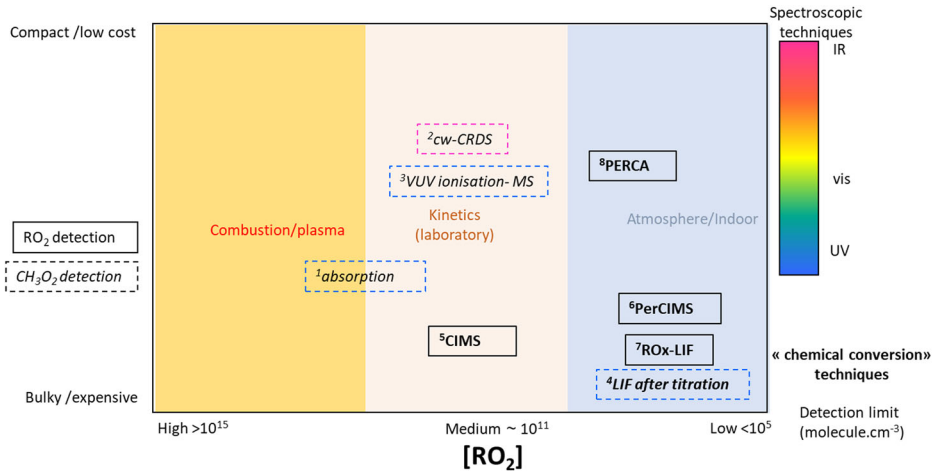

Figure 4. Techniques currently used to quantify individual or sum of RO_2 in reactive systems. Techniques for CH_3O_2: [1]Laser Flash photolysis coupled with UV-time resolved absorption detection[81] [2]Time-resolved continuous-wave Cavity Ringdown Spectroscopy[82] [3]Vacuum ultraviolet radiation of combined with time-resolved mass spectrometry[83] [4]Laser-Induced Fluorescence (LIF)[71]. Techniques for sum of RO_2: [5]CIMS[84], [6]PerCIMS[75], [7]LIF[74], [8]PERCA[78].

1. ROxLIF is derived from the FAGE technique, coupling it to a conversion cell held at ~30 Torr (addition of CO and NO) to convert RO_x (RO_2+RO + HO_2+OH) into HO_2. Sufficient CO is added so that when OH is formed it is immediately converted to HO_2, which is detected in the FAGE after titration with NO[56,73,74]. Some speciation of RO_2 is possible by measuring both the total RO_2 and the total RO_2 which gives an interference in the measurement of HO_2 (mostly larger alkane RO_2 and RO_2 derived from unsaturated and aromatic species)[56].
2. PerCIMS is based on the conversion of RO_2 into HO_2 and HO_2 into OH with the detection of OH by CIMS [75].
3. An alternative approach has been developed based on amplification/conversion (PERCA, peroxy radical chemical amplifier). PERCA is based on the conversion of RO_2 into HO_2 in the presence of a large concentration of CO and NO. HO_2 is then involved in a chain reaction in which HO_2 and OH are interconverted leading to the oxidation of NO to NO_2, which is then quantified by LIF [43], chemiluminescence [76], CRDS [77], or CAPS (cavity attenuated phase shift spectroscopy)[78,79]. Some more recent versions of a PERCA use ethane rather than CO for the chain amplification chemistry[78,80].

Figure 4 summarizes the specifications of these methods.

2.3. Nitrous acid, HONO

Nitrous Acid (HONO) is a respirable pollutant known to convert secondary amines *in vitro* to carcinogenic nitrosamines[85,86]. In addition, it can directly initiate DNA crosslinks and is expected to have mutagenic properties. Indoors, HONO is formed

following combustion, as well as by heterogeneous dark and photochemical reaction of NO_2 and is an important radical source indoors. Gómez Alvarez et al.[2] experimentally proved for the first time that photolysis of HONO was possible indoors, i.e., that the range of wavelengths that penetrate through windows could photolyze HONO yielding concentrations of OH radicals that were comparable to outdoor levels. Uptake of NO_2 to indoor surfaces can result in the heterogeneous formation of nitrous acid (HONO) by various mechanisms [87–90].

HONO mixing ratios of up to 100 ppb have been observed indoors[2,3,91–105]. The highest values measured are related to combustion processes. Under conditions where a direct source of HONO, such as a combustion appliance, is not active, mixing ratios are typically less than 10 ppb, which is still much higher than in the ambient atmosphere [2,106].

Due to the wide range of reported HONO levels (<1-100 ppb), instruments used for indoor studies should have a large dynamic range. In addition, since the indoor atmosphere can be a very complex reaction mixture including ambient pollutants (NO_x, O_3, VOCs), specific indoor pollutants (e.g., cleaning products, air fresheners, cooking emissions) and their degradation products, HONO instruments should be also selective and almost free of interferences. Furthermore, to study fast variations of indoor HONO levels, such as during cooking events, the instruments should have a time resolution at least in the low minutes range. Finally, HONO instruments should be compact to minimize disruption in indoor spaces.

Early studies using simple carbonate denuders or filter techniques did not fulfill all these requirements (e.g., [91–95,99,100,102,107]). These approaches have a low time resolution and are affected by interferences like NO_2.

Other indoor HONO studies used a modified NO_x analyzer to allow simultaneous quantitative measurements of HONO [3,92,96,107]. The HONO inlet of the instrument consists of a gas denuder (GD) channel and a bypass (BP) channel inserted upstream of the NO_x analyzer. The GD removes gaseous acids, including HONO, using a sodium carbonate coated annular denuder which does not remove NO and NO_2. Air sampled through the BP channel contains NO_2 and HONO; both molecules are converted to NO by the molybdenum catalyst [3,103,108,109]. A Teflon solenoid three-way valve enabled the sampling of GD (NO and NO_2 only) and BP (sum of NO, NO_2 and HONO, $\sum(NO_X + HONO)$) air alternating at 5 min intervals. However, this technique is not very specific since other acidic NO_y species (e.g., HNO_3) besides HONO are also removed by the carbonate denuder.

Večeřa et al. [101] used a wetted wall effluent diffusion denuder, in which water flows down on a modified interior wall of a borosilicate glass tube while sample air moves upward in countercurrent flow. The effluent liquid was debubbled and the anionic constituents were preconcentrated. The separated ions flowed through a cadmium cell to reduce NO_3^- to NO_2^-, which was detected by the Griess-Saltzman reaction. Following a 3-minute reaction time, the product dye was detected based on its absorption at 555 nm. For a 50 cm wet effluent diffusion denuder, essentially quantitative collection efficiency was observed for both HONO and HNO_3.

Differential Optical Absorption Spectroscopy (DOAS) was used in the first HONO indoor studies[98]. DOAS is fast, sensitive and selective, but indoor set-ups are cumbersome since a long path absorption system (like a White cell) is needed for high sensitivity. Thus, this technique has not been used in more recent studies.

High time resolution based on incoherent broadband cavity-enhanced absorption spectroscopy (IBBCEAS) was used for the simultaneous measurements of HONO and NO_2 [110,111]. Duan et al.[111] found measurement precisions (2σ) for HONO and NO_2 of about 180 and 340 ppt in 30 s, respectively. A field inter-comparison was carried out at a rural suburban site in Wangdu, Hebei Province, China. The concentrations of HONO and NO_2 measured by IBBCEAS were compared with a long optical path absorption photometer (LOPAP) and a NO_x analyzer (Thermo Fisher Electron Model 42i), and the results showed very good agreement, and good correlation with slopes of $0.941 \pm 00{,}0069$ and $0.964 \pm 0{,}0042$ for HONO and NO_2 respectively and correlation coefficients (R^2) of HONO and NO_2 being ~0.89 and ~0.95, respectively. In addition, vehicle deployments were also tested to enable mobile measurements of HONO and NO_2, demonstrating the promising potential of using IBBCEAS for sensitive, accurate and fast simultaneous measurements of HONO and NO_2 in the future.

Laser-photofragmentation laser-induced fluorescence (LP-LIF) has recently been applied to the indirect measurement of HONO with good sensitivity. The approach taken is to photolyze HONO and detect its OH photofragments. Bottorff et al.[112] have used this approach to measure HONO and OH in forests, urban settings, and indoors.

Mass spectroscopic techniques have been used in a few HONO indoor studies. For example, HONO can be measured with Atmospheric Pressure Interface Chemical Ionization Mass Spectrometry (API-CIMS) using chloride reagent ion chemistry [103]. In a study by Collins et al.[97], HONO was detected indoors using a High-Resolution Time-of-Flight Chemical Ionization Mass Spectrometer (HR-ToF-CIMS) after reaction with the acetate (CH_3COO^-) reagent ion. MS techniques are fast, sensitive, and can be selective when well-designed. The humidity dependence of the sensitivity by formation of water clusters has to be carefully calibrated for the CIMS technique[113]. MS instruments are not compact but still have the potential for standard use in indoor studies.

In more recent indoors studies, the LOPAP (Long-Path Absorption Photometer) has frequently been used for real time measurements of HONO [114–118]. This instrument fulfills the criteria mentioned above: a time resolution of a few minutes, high sensitivity and high dynamic range (from low ppt to ppm level), selective detection and a compact design. Since the instrument uses liquid reagents, it is not well-suited for very long-time network measurements. Table 3 summarizes results from some indoor HONO studies performed in different regions with different techniques and sample integration times (concentration levels, instrumentation used, type of indoor environment and location) using either online measurement techniques or offline analysis of collected samples.

2.3.1. HONO intercomparison campaigns

There have been several intercomparison campaigns of HONO measurements and instrumentation and the main findings are summarized in Table 4. This section is to provide general performance parameters for the most relevant instrumental techniques that have been used to quantify HONO concentrations, to aid in the selection of suitable techniques for future campaigns. LOPAP is particularly suitable for the determination of HONO in the indoor environment. It has been subjected to extensive tests through intercomparison exercises and has been compared to absolute techniques, i.e., spectroscopic instrumentation like DOAS, for which deployment in the indoor environment can

Table 3. Examples of indoor HONO studies.

Location	Building Type	Avg ± SD [ppb]	Range [ppb]	Technique	Reference
Reactions of NO_2 with water vapor in indoor environment	Chamber study: Reactivity and kinetics study of NO_2 with water vapor	(0.25 ± 0.04) ppb HONO min^{-1} per ppm NO_2 (first order rate kinetics)	15 ppb HONO per ppm NO_2 (Steady state)	DOAS	[98]
Chicago and Meriland	Two research houses: Residential with unvented gas space heaters	40 (24 h average)	0-100	Chemiluminescent NO_x monitor + carbonate denuder	[3]
Rome, Italy	Residential	Night: 14.3	9.9-20.8	Chemiluminiscence with switchable Na_2CO_3 scrubber	[107]
Lubbock, TX (USA)	University Laboratory	N/A	0-3	Wet effluent Diffusion Denuder (WEDD) with Low-pressure Ion Chromatography-Postcolumn Reaction Detection	[101]
Alburquerque, NM (USA)	Residential	4.7 ± 2.3	1.8-8.1	Carbonate denuder + filter pack	[102]
Ohio (USA)	Residential (combustion sources)	N/A	0-18	Atmospheric Pressure Chemical Ionization Mass Spectrometry (APCI MS)	[103]
Lubbock, TX (USA)	Residential (combustion processes)	N/A	20-90	WEDD	[104]
Brazil	Commercial	4.3 ± 2.8	1.0-8.8	Carbonate-impregnated filter	[105]
Eastern USA	Residential	4.0 ± 2.8 (summer) 5.45 ± 3.75 (winter)	0-11.3	Carbonate/ glycerol denuder	[92]
Florence (Italy)	Galleria degli Uffizi	4.8	2.6-7.3	Carbonate denuder	[91]
Chamber experiment	Investigation on HONO formation on Teflon, wallpaper, carpet (50, 70% RH)	N/A	Up to 12 ppb for 140 ppb NO_2 (air exchange rate= 0.53 h^{-1})	Chemiluminescence + carbonate denuder	[119]
California, USA	Residential	4.6	0-21	Passive sampler; carbonate-impregnated filter	[93]
Cairo, Egypt	Residential	3.67 (summer) 6.8 (winter)	1.3-7.3 1.6-12.5	Carbonate denuder	[94]
	Commercial	1.24 (summer) 1.42 (winter)	0.52-2.13 0.61-2.21		
Gwangiu, Korea	Residential	1.4	0.3-9	Online liquid trap/ luminol detection	[120]
Gwangiu (Korea)	Residential (occupied apartment)	2.1	0.2-15.2	Online liquid trap/ luminol detection	[121]
Marseille (France)	School	5.6	<12	NITROMAC aqueous scrubber-HPLC-UV instrument	[2]
Bern, Geneva (Switzerland) Prague, Teplice (Czech Republic)	Libraries	1.9		Diffusion sampler filter pack	[95]
Syracuse, NY, USA	Residential	4.3 ± 2.2	3-7	Chemiluminiscence with switchable Na_2CO_3 scrubber	[96]
Toronto, ON, Canada	Residential	5.3 ± 1.1	3.0-14.2	Online acetate chemical ionization mass spectrometry	[97]
East Anglia, UK	Residential	3.19	2.05-5.09 0-20.55	Passive sampler	[117]

Table 4. Intercomparison of analytical techniques/instrumentation for the determination of HONO.

Techniques/Instruments intercompared	Summary of results	Reference
DOAS/Annular Denuder (AD)	Good agreement during night, AD ≫DOAS during day	[122]
DOAS/ AD	Good agreement and correlation, but ca. 0.7 ppb offset	[123]
DOAS/Chemiluminescence	Good agreement	[124]
DOAS/Rotated Wet Annular Denuder (RWAD)	Good agreement during night, AD ≫DOAS during day	[125]
LOPAP/DOAS (EUPHORE)	Good agreement for complex conditions (Diesel exhaust/dark)	[126,127]
Parallel Plate Wet Denuder (PPD) (pH = neutral), (RWAD) (pH =9)	Reasonable agreement, often higher HONO for the RWAD. Higher interferences of the RWAD at high pH and /or incomplete sampling of the PPD at lower pH	[128]
Air-dragged Aqua-Membrane-Type Denuder with Fluorescence Detection/Dry Denuder/DOAS	Reasonable agreement between the fluorescence detection and the denuder, good agreement of fluorescence and DOAS during night, but higher than DOAS during day	[129]
DOAS/LOPAP	Excellent agreement in a smog chamber under complex conditions and in a field campaign (urban background, Milan)	[130]
DOAS/Wet Effluent Diffusion Denuder (WEDD)(PPD)	Reasonable agreement between both instrument, higher HONO by the WEDD during daytime	[131]
DOAS/Mistchamber- Ion Chromatography (IC)	Good agreement during night, Mistchamber ≫DOAS during day	[132]
Stripping coil- (IC)/LOPAP	Good agreement	[133]
DOAS/Stripping coil-absorption photometry (SC-AP)/LOPAP/MC-IC/ Quantum Cascade Tunable Diode Laser (QC-TILDAS)/Ion Drift-Chemical Ionization Mass Spectrometry (ID-CIMS)	Reasonable agreement between the instruments, except for the ID-CIMS which shows significant higher HONO	[134]
Modified LOPAP (selenoid pumps instead of peristaltic pump)/ commercial LOPAP,	Modified LOPAP > commercial LOPAP, potential reason 5 m long inlet of the modified LOPAP	[135]
NitroMAC/LOPAP	Excellent agreement in a smog chamber, NitroMAC > LOPAP in the atmosphere	[136]
Incoherent Broadband Cavity-Enhanced Absorption Spectrometer (IBBCEAS)/LOPAP	Excellent agreement	[111]
Stripping coil-IC/LOPAP/CEAS	Good agreement between all techniques	[137]
RWAD (Monitor for Aerosols and Gases in Ambient Air, MARGA)/LOPAP	MARGA > LOPAP	[138]
Commercial LOPAP/Custom Build LOPAP/2x IBBCEAS/ToF-CIMS	High correlation but significant differences between the instruments, reasons were not clarified, potential spacial variability, different inlet position	[139]

pose significant hurdles. For higher indoor levels (>several hundred ppts) the IBBCEAS technique is also a suitable candidate, since these instruments are also compact, fast and selective.

2.4. Reactive chlorine and precursors

The highly reactive Cl atom is a powerful oxidant of both organic and inorganic compounds and can be an important driver of atmospheric chemistry in both indoor and

outdoor environments. The reactive nature of atomic Cl means that its concentrations are too low to be directly measured in the lower atmosphere. Measurements of chlorine-containing species, however, can give us significant insight into both the scale of atomic Cl oxidation and the production of known respiratory irritants (e.g., NCl_3).

These chlorinated gas phase compounds can be broadly classified into two groups — either organic/amine or inorganic compounds. Most chlorinated-organic compounds are stable with respect to tropospheric degradation processes (e.g., photolysis and OH reaction), and are either directly emitted or formed as oxidation products of Cl atom reactions with hydrocarbons. In contrast, inorganic chlorine compounds (e.g., HCl, HOCl, $ClNO_2$) can release Cl atoms during their tropospheric cycling and can be considered Cl atom reservoirs. These inorganic compounds are often formed via heterogeneous processes, which are thought to be important drivers of indoor chlorine chemistry [6,8,140].

Observations of chlorinated organic compounds provide useful information as tracers of Cl atom oxidation of hydrocarbons, and the detection of chloramines is useful both as an indicator of their production mechanisms and their direct health impacts. Measurements of inorganic chlorine compounds are key to improving our understanding of the dominant chlorine production and cycling mechanisms. Much of our understanding of chlorine chemistry comes from the study of stratospheric ozone chemistry, but many of the observational techniques used to study the stratosphere (e.g., satellite differential optical absorption) are not suitable for the indoor environment. However, recent developments in both mass-spectrometry and optical techniques make possible the in-situ study of complex chlorine chemical cycles. Table 5 summarizes in-situ observational techniques that have been, or could be, used for the study of chlorine chemistry in the indoor environment.

2.5. NO_3 and N_2O_5

NO_3 is a major nocturnal oxidant in outdoor air formed through the relatively slow reaction between NO_2 and O_3 [149]:

$$NO_2 + O_3 \longrightarrow NO_3 + O_2$$

Further reaction with NO_2 reversibly produces N_2O_5, which acts as a reservoir for NO_3:

$$NO_2 + NO_3 \rightleftharpoons N_2O_5$$

Rapid photolysis by visible radiation (photolysis lifetime of a few seconds in direct sunlight) suppresses NO_3 concentrations under daylight conditions. NO_3 reacts rapidly with unsaturated VOCs and can lead to SOA formation. Heterogeneous hydrolysis of N_2O_5 on surfaces of solids or particles is an important loss route for nitrogen oxides, producing nitric acid. Heterogenous N_2O_5 reactions with aerosol and surface chloride produce $ClNO_2$, a photolabile source of Cl and NO_2.

Absorption spectroscopy has been the most commonly used approach for detecting NO_3 based on its intense absorption band at 662 nm, allowing sensitive real-time measurements [150]. For in situ measurements, optical cavities are applied using ringdown or cavity-enhanced absorption spectroscopy. Monochromatic (laser) or broadband light

Table 5. Techniques and measurement characteristics for chlorine species.

Technique	Compound/s	**Typical Limit of Detection** [pptv]	Time resolution (indicative)	Practical considerations	Example reference
Gas chromatography-mass spectrometry	Chlorinated organics (e.g., CFCs, $CHCl_3$, CCl_4)	> 0.5	10 — 30 min	Majority of studies use sampling followed by pre-concentration and off-line analysis, although on-line detection is possible with low time resolution (10 min — 1 h)	[140]
Proton-transfer reaction time-of-flight mass spectrometer	Chloramines (e.g., $NHCl_2$, NCl_3)	1	1 s	Highly sensitive, high time resolution instrument that can simultaneously measure multiple compounds. But instrument is expensive and complicated to calibrate/operate. Note that simultaneous measurements of $NHCl_2$ and NCl_3 by I-CIMS and PTR by Mattila et al.[8] reported concentration discrepancies of several orders of magnitude	[8]
Iodide chemical ionization mass spectrometry (I-CIMS) / time-of-flight CMIS (I-tof-CIMS)		< 10	1 s	Highly sensitive, high time resolution instrument that can simultaneously measure multiple compounds of interest, but instrument is expensive and complicated to calibrate/operate. Also requires radioactive source. Interferences can be issues, especially from small molecules, which can be formed via fragmentation within the instrument. This has been specifically noted for ClO[8].	[6,8]
	Chlorinated oxygenated organics	1	1 s		
	HOCl	30	1 s		
	$ClNO_2$	1	1 s		
	Cl_2	3	1 s		
	Cl_2O	0.2	1 s		
	ClO	3	1 s		
Chemical conversion resonance fluorescence		4	16 s	Complex custom instrumentation that is no longer in frequent use.	[141]
Laser Absorption spectroscopy	HCl	10	1 s	Relatively simple methodology and optical nature makes it selective. HCl is difficult to sample due to wall effects. Specifications are for instrument presented by Halfacre et al. at EGU 2020. Citation is for an older instrument with significant inlet effects.	[142]
Cavity ring-down spectroscopy		18	30 s	Compact instrument. Humidity dependant response time due to wall interactions	[143]
Off-axis integrated cavity output spectrometer (OA-ICOS)		78	30 s	Compact and lightweight instrument. Has been deployed as part of a stratospheric balloon payload. Has not been demonstrated for tropospheric humidities and artifacts	[144]
Denuder or filter collection		200	30 min— 24 h	Offline analysis method. Poor time resolution but relatively simple	[145]

(*continued*)

Table 5. Continued.

Technique	Compound/s	Typical Limit of Detection [pptv]	Time resolution (indicative)	Practical considerations	Example reference
followed by offline ion-chromatography				sampling, without the need for large complex in-situ instrumentation	
Iodide chemical ionization mass spectrometry (I-CIMS) / time-of-flight CMIS (I-tof-CIMS)		30	30 s	See above for I^- CIMS	[146]
Acetate chemical ionization time-of-flight mass spectrometry		2	1 min	Highly sensitive, high time resolution instrument, but expensive and complicated to calibrate / operate. Acetate ion inlet chemistry also less widely used than I^-	[147]
SF_6^- chemical ionization mass spectrometry		2	30 s	Highly sensitive, high time resolution instrument, but expensive and complicated to calibrate / operate. SF_6^- ion inlet chemistry also less widely used than I^-	[148]

sources may be used. Laser-based methods require additional measures to account for absorption by NO_2 and O_3 and scattering by particles. Inlet filters can be used to remove particle extinction, but must be changed regularly to avoid variable NO_3 losses with aging [151]. The rapid titration of NO_3 with NO:

$$NO_3 + NO \longrightarrow 2NO_2$$

is often used to establish a baseline extinction.

Broadband methods use spectral analysis over tens of nanometers to retrieve the absorption and hence concentration of NO_3. Interfering absorptions are identified through spectral fitting; however, water can complicate spectral retrieval because water absorption lines are too narrow to be resolved by a spectrograph and measured spectra diverge from the Beer-Lambert law [152]. Calibrating the response of broadband instruments is also more complex than for CRDS systems. Many outdoor (often airborne) studies now use the optical cavity methodology.

N_2O_5 is indirectly detected as NO_3 via thermal decomposition at elevated temperatures in the sample inlet. A single, extractive instrument with heated and unheated inlet channels can therefore be used to detect both NO_3 and N_2O_5. Although most optical cavity instruments draw the air sample through an enclosed optical cavity, broadband open path systems based on CEAS may have potential for indoor measurements, although N_2O_5 quantification is not possible with this configuration [153,154].

Alternative methods include thermal dissociation-chemical ionization mass spectrometry (TD-CIMS) to quantify the sum of NO_3 and N_2O_5 using ionization by the I^- ion [155,156]. Laser-induced fluorescence detection of NO_3 has been demonstrated to a 1σ sensitivity of about 4 pptv over a 10 min period [157,158]. The LIF is less sensitive than absorption-based methods and has not been extensively pursued for detecting NO_3/N_2O_5. A flow tube reactor combined with adsorbent tube sampling and analysis using

Table 6. Measurement type and performance characteristics of instrumentation to measure NO_3 and N_2O_5.

Technique	Compound	Typical Limit of Detection (2σ) [pptv]	Time resolution [s]	Description	Reference
CRDS	NO_3				[160]
CRDS	NO_3	0.5	5		[161]
	N_2O_5	0.5	5		
CW-CRDS	N_2O_5	2.4	24	CW-CRDS system with heated inlet	[162]
	NO_3	1.7	24	Estimated for NO_3	
BB-CRDS	NO_3	1	100		[152]
	N_2O_5	1	100		
BBCEAS	NO_3	0.5	10		[163]
IBBCEAS	NO_3	2.7	60	Open path across chamber, 4 m	[153]
	NO_3	3	30	Open path, 0.84 m cavity length	
IBBCEAS	NO_3	4	10	Open path across chamber, 0.82 cm cavity length	[164]
CRDS	NO_3	4.6	2.5	Compact, inexpensive, 2 channels for NO_3 & N_2O_5	[165]
	N_2O_5	6.2	2.5		
IBBCEAS	NO_3	3	100	Compact and low-cost instrument. NO_2 & NO_3 detection at 625 nm. LoD is stated as upper limit, but unclear whether LoD defined as 1σ, 2σ, 3σ	[166]
BBCEAS	NO_3	1.4	1	For airborne measurements. Two channel instrument	[167]
	N_2O_5				
Open path IBBCEAS	NO_3	3	30	Open path system	[154]
TD-CIMS	$NO_3 + N_2O_5$	8	1	Main focus on peroxyacyl nitrates	[155]
TD-CIMS	$NO_3 + N_2O_5$	7	60	Use of I^- ionization. Used in field	[156]
LIF	NO_3	76	60		[158]
	N_2O_5	76	60		
LIF	NO_3	8	600		[157]
	N_2O_5	12	600		

thermal desorption-gas chromatography was used for the first experimental measurements of indoor NO_3/N_2O_5 chemistry but the system is complex and time resolution is poor [159].

Performance characteristics of instruments measuring NO_3 and N_2O_5 are given in Table 6. Instrument intercomparison studies have shown good agreement between the different absorption methods [168,169].

2.6. Criegee intermediates

Criegee Intermediates (CIs), also known as zwitterionic intermediates or carbonyl oxides, have been the center of growing interest over the past decade due to their

potential role in the oxidative capacity of the atmosphere and specifically in SO_2 oxidation and secondary aerosol formation.

Outdoor concentrations ranging from 10^4 to 10^5 molecules cm^{-3} have been estimated from modeling studies for the sum of atmospheric Criegees[170]. This range of values is consistent with indirect observations indicating a mean concentration of approximately 5×10^4 molecules cm^{-3} during the HUMPPA-COPEC 2010 (forested area) and HOPE 2012 (rural area) field campaigns[171]. The pool of atmospheric CIs is complex due to (i) the multitude of unsaturated VOCs that can react with ozone in the atmosphere and (ii) the potential formation of syn- and anti-conformers. Both the complexity of the CI mixture and their presence at low concentrations put stringent demands on analytical techniques in terms of sensitivity and selectivity.

While no technique is currently available for atmospheric measurements of CI, some direct and indirect approaches have been developed in the laboratory to characterize the chemical structure of small CIs (C_1-C_6) and to study their kinetics. Techniques for direct detection of specific CIs include photoionization mass spectrometry, spectroscopic approaches in the ultraviolet, infrared and microwave regions, and chemical ionization mass spectrometry [172,173]. An indirect technique relying on the stabilization of CIs using spin trap molecules and their subsequent detection by mass spectrometry was also proposed[174–176]. In addition to these laboratory techniques, a few instruments designed for hydroxyl radical measurements in the atmosphere have shown potential to detect unspeciated CIs[171,177]. First, we briefly describe techniques designed to investigate the structure and the kinetics of CIs in the laboratory and we then discuss OH field instruments that may be capable of detecting CIs in the atmosphere.

2.6.1. Detection techniques employed in the laboratory for fundamental research

1. *Photoionization mass spectrometry (PIMS):* Taatjes et al.[178] and Welz et al.[179] demonstrated that PIMS can be used for detecting individual CIs in simple chemical mixtures. The authors employed the tunable vacuum UV light from the ALS synchrotron at Berkeley National Laboratory to perform kinetic experiments on the simplest CI, formaldehyde oxide (CH_2OO). A subsequent study from the same group highlighted that some selectivity can also be achieved between anti- and syn-conformers of acetaldehyde-oxide (CH_3COO) on the basis of their difference in ionization energy[180]. This technique was extended to the detection of acetone-oxide ($(CH_3)_2COO$)[181].
2. *UV-Vis absorption spectroscopy:* This technique was used by several groups for the detection of formaldehyde-oxide, acetaldehyde-oxide, methylvinylketone-oxide, and methacrolein-oxide, taking advantage of their specific absorption features[173,182]. Sheps et al.[183] reported that syn- and anti-conformers of acetaldehyde-oxide can be distinguished in this range of wavelengths. Instrumentation used to monitor CIs during laboratory experiments are single pass cell/LED, multipass cell/Ti:Saphire laser, CEAS, and CRDS [173].
3. *IR absorption spectroscopy*: Several studies used IR absorption spectroscopy to detect different conformers of acetaldehyde-oxide, acetone-oxide, methylvinylketone-oxide, and methyl-ethyl Criegee intermediate (MECI)[173,184,185]. A higher degree of selectivity than in the UV region can be achieved if high-resolution IR

sources are used. The detection of CIs is performed using broadband FTIR, high-resolution CW-QCL, and action spectroscopy [173].

4. *Microwave spectroscopy*: This technique was used under molecular beam conditions to investigate the molecular structure of CIs and their kinetics, including various isotopologues of formaldehyde oxide, syn- and anti-conformers of acetaldehyde-oxide, and acetone-oxide [173].
5. *Spin trap/Chemical Ionization Mass Spectrometry:* Gioro et al. [174,175] proposed an online method relying on the stabilization of CIs using a spin trap molecule (DMPO - 5,5-dimethylpyrroline-N-oxide) and the quantification of the CI-spin trap adducts by Proton Transfer Reaction-Mass Spectrometry (PTR-MS) using H_3O^+ reagent ions. Combining high resolution mass spectrometry with the selective nature of the DMPO-CI reaction has the potential to provide the discrimination needed to speciate non-isobaric CIs in complex chemical mixtures. The authors reported detection of CIs generated from ozonolysis of biogenic and anthropogenic alkenes with a detection limit of approximately 7×10^8 molecules cm^{-3} (10 s integration time) for α-pinene-derived CIs. More recently, Zaytsev et al. [176] also reported the use of DMPO and other spin trap species (HFA: Hexafluoroacetone, TEMPO: (2,2,6,6-tetramethylpiperidin-1-yl)oxyl) with PTR-MS using H_3O^+ and NH_4^+ reagent ions. The authors reported detection limits for acetone-oxide of 1.4×10^7 molecules cm^{-3} and 3.4×10^7 molecules cm^{-3} at a time resolution of 30 seconds using HFA/H_3O^+ and DMPO/NH_4^+, respectively.
6. *Chemical Ionization Mass Spectrometry*: Berndt et al. [186] demonstrated that CIs can also be directly detected by CIMS as adducts using reagent ions such as protonated ethers (tetrahydrofuran, diethyl ether) for formaldehyde-oxide and protonated amines (n- and tert-butylamine, diethylamine) for cyclohexene-derived C6-CIs. The authors stressed that selective detection of CIs from other isomeric compounds is possible through careful selection of reagent ions. However, selective detection of CIs in the complex mixture of ambient trace gases has yet to be demonstrated. Detection limits ranging from 10^4 to 10^5 molecules cm^{-3} were observed during kinetic experiments using a CI-APi-TOF (Chemical Ionization – Atmospheric Pressure interface – Time Of Flight) instrument at a time resolution of 10 min.

2.6.2. Field deployable instruments and atmospheric measurements of CIs

The deployment of instruments capable of measuring the atmospheric hydroxyl radical (OH) has provided surprising observations over the past decades, indicating that species other than OH were detected during specific steps of the OH measurement sequence. Indeed, zeroing approaches implemented by CIMS, [177] and FAGE, [28,171]) instruments have highlighted the presence of reactive species capable of oxidizing SO_2 in CIMS instruments or capable of producing OH in the low pressure sampling cell of FAGE instruments. Further investigations indicated that the behavior of these unidentified species is consistent with the known CI chemistry, which suggests that a substantial fraction of these unidentified species could be CIs. The extent to which "background" signals from both CIMS and FAGE instruments are connected to ambient CIs is not

clear and further investigation is necessary to determine whether these techniques could be used to provide integrated measurements of the pool of ambient CIs.

While a large number of techniques have been used in the laboratory to characterize the molecular structure of CIs and their kinetics, it will be challenging to transfer these techniques for indoor environments due to the sensitivity and selectivity required. Indeed, these techniques were employed on experimental systems where large concentrations of CIs (likely higher by several orders of magnitude than in the atmosphere) can be generated in simple chemical mixtures, with a lower number of potentially interfering species than in the atmosphere. The most promising approach, which was shown to reach detection limits that are close to estimated ambient CI concentrations, is CIMS [186], which has already been used for monitoring other reactive species such as the hydroperoxyl radical (HO_2) [62] and HOMs [187]. The quantification of atmospheric CIs will also require the development of calibration apparatus capable of generating known concentrations of specific CIs [171].

2.7. Glyoxal and methylglyoxal

Photolysis of dicarbonyl compounds, specifically glyoxal (CHOCHO, GLY) and methyl glyoxal ($CH_3C(O)CHO$, MGLY), is the main initiation route that produces HO_2 and RO_2 [188]. This route has been verified several times in the outdoor environment. It also operates efficiently in the indoor environment and can even be enhanced under certain circumstances such as cleaning or use of air cleaners [4]. GLY and MGLY are produced in the atmosphere by several processes, including oxidation of VOCs (particularly biogenic species) [189], anthropogenic photo-oxidation of aromatics in the presence or absence of NO_x [190–195], pyrogenic sources [196–200], and via chemical routes such as dicarbonyl formation from Criegee biradicals [201].

The main sources of GLY and MGLY in the indoor environment are diverse, and most of them are also observed outdoors (e.g., oxidation of aromatic species). Other routes more specific to the indoor environment would be formation via metabolic processes since they are formed endogenously in numerous enzymatic and nonenzymatic reactions [202–207]. Particularly important to the indoor environment is their formation by ozonolysis of terpenes, found in cleaning products and fresheners. The ozonolysis of squalene is closely related to the presence of occupants because squalene is an important component of human skin oil. Given the high degree of unsaturation in squalene, tertiary and higher-order reaction products can be generated and sequential ozone attack generates bifunctional secondary products that contain carbonyl, carboxyl, or α-hydroxy ketone terminal groups [208]. The major bifunctional products are the four dicarbonyls: 4-oxopentanal (4-OPA), 1,4-butanedial (succinic dialdehyde), 4-methyl-8-oxo-4-nonenal (4-MON), and 4-methyl- 4-octene-1,8-dial (4-MOD) produced by attack at the bonds.

2.7.1. Measurement of indoor glyoxal and methylglyoxal

GLY and MGLY can be measured by various techniques: infrared (IR) absorption spectroscopy [209,210], ultraviolet-visible (UV-Vis) absorption spectroscopy[211–214], chromatographic analysis of derivatization by O-(2,3,4,5,6-pentafluorobenzyl)-hydroxylamine (PFBHA) or dinitrophenylhidrazyne (DNPH) followed by mass spectrometry or flame

ionization, and phosphorescence [215,216]. CIMS (using H_3O^+, O_2^+ or NO^+ reagent ions) has also been used to detect MGLY [217–220].

Most measurements of GLY and MGLY have used derivatisation techniques and a variety of sampling methods with off-line GC analysis with different detectors, GC/MS or HPLC. The most extensively investigated source of GLY and MGLY and other dicarbonyls indoors is from ozonolysis of terpenes in cleaning products, air fresheners, and ventilation systems. Derivatisation techniques have mainly been used for this analysis, and hundreds of papers can be found in the literature on this topic. Table 7 lists example studies that applied derivatization with off-line chromatographic analysis to illustrate the most common sources of GLY, MGLY (and in some studies, several other dicarbonyls) that have been studied in the indoor environment.

Szulejko and Kim [233] authored a general review of derivatization techniques for determination of carbonyls in air and provided a list of selected derivatising agents. The most common are O-(2,3,4,5,6-pentafluorobenzyl)hydroxylamine hydrochloride (PFBHA) 2,4-dinitrophenylhydrazine (DNPH). Studies by Ham et al. [228] and Jackson et al. [234] used TBOX, o-tert-butylhydroxylamine hydrochloride as derivatizing agent. A fluorogenic reagent, dansylhydrazine (DNSH) provide hydrazones that can be analyzed by fluorescence, which enhances the sensitivity and selectivity of the technique. Zhang et al. [235] used this method to develop a Personal Aldehydes and Ketones Sampler (PAKS). Other applications have been detection of GLY (and other toxic carbonyl compounds) in cigarette smoke [236] by derivatizing reactive carbonyl compounds into stable nitrogen-containing compounds (pyrazoles for β-dicarbonyl and α,β-unsaturated aldehyde; and quinoxalines for α-dicarbonyls), followed by quantitative detection using gas chromatography with a nitrogen phosphorus detector.

Indoor environments have access obstacles and space constraints that do not influence outdoor measurements. Techniques that have been used for indoor measurements of GLY and MGLY are mostly easy to deploy techniques that do not require bulky equipment or that involve only the sampling of gases or particles followed by offline analysis. There are a few exceptions like the HOMECHEM campaign [237] or the SURFIN campaign in a school classroom in Marseille [2]. For these reasons, the intercomparison exercises carried out in simulation chambers constitute a useful basis to discuss the different measurement techniques for GLY and MGLY.

Thalman et al. [238] carried out an intercomparison of different techniques for the measurement of GLY, MGLY and NO_2 in the NCAR and EUPHORE chambers (see Table 8). Excellent linearity was attained by all instruments/techniques under idealized conditions (pure GLY or MGLY, $R^2 > 0.96$) and in complex gas mixtures characteristic of dry photochemical smog systems (o-xylene/NOx and isoprene/NOx, $R^2 > 0{:}95$; $R^2 \sim 0.65$ for offline Solid Phase Micro Extraction, SPME, measurement of MGLY). The correlations were more variable at higher humidity (RH > 45%) for MGLY ($0.58 < R^2 < 0.68$) than for GLY ($0.79 < R^2 < 0.99$). Intercepts of correlations were generally below the instruments' experimentally determined detection limits and slopes varied by less than 5% for instruments that could also simultaneously measure NO_2. For GLY and MGLY the slopes varied by less than 12 and 17% (both 3σ) between direct absorption techniques (i.e., calibration from knowledge of the absorption cross section). Larger variability was found among in situ techniques that employed external calibration

Table 7. Synopsis of some of the most relevant indoor studies using derivatization followed by off-line chromatographic analysis that have determined glyoxal and/or methylglyoxal as a result of representative indoor activities.

Derivatising agent	Sampling method	Indoor activity	Precursor	Instrument	Carbonyls/Dicarbonyls detected	Reference
PFBHA	FLEC Automation and Control System (FACS)	Cleaning	α-terpineol + O_3	GC/MS	GLY, MGLY 4-oxopentanal, 4-methylcyclohex-3-en-1-one, 6-hydroxyhept-en-2-one, 3-(1-hydroxy-1-methylethyl)-6-methylcyclohex-2-en-1-one), 5-(1-hydroxy-1-methylethyl)-2-methylcyclohex-2-en-1-one	[221]
PFBHA	Captured in solution) on glass plate surface)	Skin (emissions due to dwellers)	Squalene + O_3	GC-Ion Trap Mass Spectrometry	GLY 6-methyl-5-hepten-2-one (6MHO), 4-oxopentanal (4OPA), geranyl acetone, 5,9,13-trimethyltetradeca-4,8,12-trienal	[222]
PFBHA	Samples drawn through a 6.4 mm Teflon Swagelok fitting attached to a 65 L Teflon chamber	Cleaning	α-Terpineol + NO_3^-	GC/MS	GLY, MGLY acetone, 6-hydroxyhept-5-en-2-one, 4-(1-hydroxy-1-methylethyl)-1-methyl-2-oxocyclohexyl nitrate, 5-(1-hydroxy-1-methylethyl)-2-oxocyclohexyl nitrate, 1-formyl-5-hydroxy-4-(hydroxymethyl)-1,5-dimethylhexyl nitrate, 1,4-diformyl-5-hydroxy-1,5-dimethylhexyl nitrate	[223]
PFBHA	PDMS/DVB SPME	Cleaning	Citronellol + O_3	GC/MS	GLY, MGLY acetone, 6-hydroxy-4-methylhexanal	[224]
PFBHA	four bubblers with frits, containing 500 ml acetonitrile each	Ventilation	α-pinene (heterogeneous reactions)	GC/MS in the positive chemical ionization mode using CH_4 as reagent gas	GLY, MGLY Several other carbonyls	[225]
PFBHA	SPME	Cleaning	terpinolene + O_3, terpinolene + NO_3^-	GC/MS	GLY, MGLY, other dicarbonyls (including some very photolabile unsaturated ones)	[226]
DNPH	Silica cartridges	Cleaning	a-pinene, camphene, b-pinene, myrcene, 3-carene, p-cymene, d-limonene, eucalyptol, g-	HPLC/MS	GLY, MGLY formaldehyde, acetaldehyde, acetone, propionaldehyde, 2-butanone (MEK), iso + n-butyraldehyde, benzaldehyde, iso-valeraldehyde, n-	[227]

(*continued*)

Table 7. Continued.

Derivatising agent	Sampling method	Indoor activity	Precursor	Instrument	Carbonyls/Dicarbonyls detected	Reference
			terpinene, terpinolene, linalool, a-terpineol		valeraldehyde, o-tolualdehyde, m-tolualdehyde, p-tolualdehyde, hexanal, 2,5-dimethylbenzaldehyde Unsaturated carbonyls: acrolein, crotonaldehyde	
O-tert-butyl-hydroxyl-amine hydrochloride (TBOX)	Water in Impinger	Cleaning,	terpinolene + O_3, terpinolene + NO	GC/MS	MGLY 4-methylcyclohex-3-en-1-one, (4MCH), 6-oxo-3-(propan-2-ylidene) heptanal (6OPH), 3,6-dioxoheptanal (36DOH). The tricarbonyl 36DOH has not been previously observed.	[228]
TBOX	Bubbler	3D printer	acrylonitrile butadiene styrene (ABS) or polylactic acid (PLA) filaments	GC/MS	GLY, MGLY Benzaldehyde, m-tolualdehyde, 2-oxopentanal	[229]
PFBHA	Methanol in Impinger	Cleaning	Terpenes (limonene, terpineol, geraniol)	GC/MS	GLY, MGLY 4-oxopentanal	[230,231]
PFBHA	Methanol in Impinger	Freshener's emissions	b-Ionone (+OH/O3)	GC/MS	GLY, MGLY	[232]

Table 8. Instrumentation used in the intercomparison of GLY, MGLY and NO_2 measurements carried out in the atmospheric simulation chambers EUPHORE (Valencia, Spain) and NCAR (Boulder, Colorado, USA). Based on Thalman et al. [238]

Instrument	Participant[a]	Species[b]
NCAR Chamber		
Cavity-Enhanced Differential Optical Absorption Spectroscopy (CE-DOAS)	CU	G,M,N
Fourier Transform Infrared Spectroscopy (FTIR)	NCAR	G,M,N
Proton transfer reaction mass spectrometry (PTR-ToF-MS)	NCAR	M
EUPHORE Chamber		
CE-DOAS	CU	G,M,N
Broadband Cavity Enhanced Absorption Spectroscopy (BBCEAS)	Leic	G,M,N
PTR-ToF-MS	Leic	M
Laser-induced phosphorescence (LIP)	UW	G,M
White-cell Differential Optical Absorption Spectroscopy (W-DOAS)	CEAM	G,M,N
FTIR	CEAM	G,M
Solid-Phase Micro Extraction-Gas Chromatography (SPME/GC-FID)	CEAM	G,M

[a]CU = University of Colorado, Boulder, USA; NCAR = National Center for Atmospheric Research, Boulder, USA; Leic = University of Leicester, UK; CEAM = CEAM, Spain.
[b]G = GLY, M = MGLY, N = NO_2.

sources (75–90%, 3σ), and/or techniques that used offline analysis. The main conclusion was that techniques now exist to conduct fast and accurate measurements of GLY at ambient concentrations, and MGLY under simulated conditions. Measuring ambient concentrations of MGLY would be desirable but remains a challenge. Recent work by Michoud et al.[239] have shown that MGLY can be measured using PTR-ToF-MS and shows reasonable agreement with the DNPH–HPLC–UV method.

In most of the reactions generating GLY and MGLY in the indoor environment other dicarbonylic products are also expected some unsaturated, highly photo-labile and short-lived (e.g., butenedial, 4-oxo-2-pentenal), and hence also powerful sources of radicals in several relevant reactions in the indoor environment for which analytical determination could be even more challenging.

2.8. Photolysis rates (J values)

To accurately determine the role of photolysis processes in indoors atmospheres, it is necessary to characterize both the natural light transmitted through windows as well as light from artificial sources, in terms of wavelength and intensity. Indeed, determining the production rate of radicals or other species by photolysis requires the photolysis rate J (in s^{-1}) of the species being photolyzed, which is given by:

$$J = \int_{\lambda min}^{\lambda max} F(\lambda) \times \sigma\ (\lambda) \times\ \varphi\ (\lambda) d\lambda$$

Here $F(\lambda)$ is the actinic flux (photons $cm^{-2} nm^{-1}\ s^{-1}$), $\sigma(\lambda)$ is the cross section of the molecule (cm^2) at the wavelength λ (nm) and $\varphi(\lambda)$ is the dimensionless quantum efficiency, i.e., the probability of photodissociation of the molecule after absorption of a photon at wavelength λ. λ_{min} and λ_{max} represent the range of wavelengths that need to be considered to cover the absorption spectrum of the molecule. $\sigma(\lambda)$ and $\varphi(\lambda)$ are spectroscopic parameters, which have been measured in the laboratory for many molecules of atmospheric interest, often as a function of pressure and temperature, and are

provided by databases such as the MPI Spectral Atlas (http://satellite.mpic.de/spectral_atlas/index.html). The production rate of the species generated by photolysis can then be calculated multiplying J with the concentration of the photolyzed species.

Spectroradiometers are able to measure actinic fluxes as a function of wavelength, which can then be combined with literature data to calculate photolysis frequencies [240]. For the measurement of photolysis rates specifically of O_3 to form $O(^1D)$, and NO_2 to form $O(^3P)$, fixed bandwidth filter radiometers can be also used [241]. A comprehensive account of the different methods is provided by Hofzumahaus [240]. Some of the different types of spectroradiometers (providing spectrally resolved data) include:

1. LICOR or Ocean optics spectrometer [10,242,243].
   Both instruments have a cosine receptor and measure irradiance. From the irradiance measurement $I(\lambda)$ at the wavelength λ (in nm), the actinic flux $F(\lambda)$ is calculated by dividing I by cosine θ, θ being the azimuth angle under conditions of direct sunshine. For conditions of indirect sunlight it is considered that the light comes from all directions (through the window and by reflection off surfaces) and is isotropic, the actinic flux is obtained by multiplying the irradiance by a factor of 2.
2. METCON spectroradiometers [9,244] .
3. PAR (photosynthetically active radiation) sensors provide integrated light intensity (400-750 nm). When calibrated by a spectrometer, these sensors can provide an integrated photon flux (irradiance) over the wavelength range 400-750 nm. As PAR sensors are compact and cheap, they can be used to map the light distribution in a room [243].

3. Future indoor measurements of radicals and radical precursors

The techniques described above for quantifying the concentrations of radicals and radical precursors illustrate the challenge of measuring highly reactive species. Below we consider the analytical and operational characteristics needed for quantifying indoor air components.

Occupied indoor spaces pose particular measurement challenges, and it may be necessary to adapt instrumentation developed for outdoor measurements to the indoor environment. Instruments must operate in relatively confined indoor spaces that might be occupied by people during the measurements. Instrumentation therefore should be as unobtrusive as possible; this includes considerations of instrumentation size and minimizing the generation of heat and noise (for example, from instrumentation pumps). Emissions of instrument chemicals and exhaust gases must also be considered and minimized.

Indoor concentrations of radicals and their precursors can differ considerably from outdoors. For example, indoor combustion sources like cooking can produce high local HONO levels, and cleaning activities can release much higher levels of chlorinated compounds than would occur outdoors. In studies where episodes of high concentration are the primary focus, this could allow instrumentation sensitivity to be slightly relaxed. In

other cases, instrumentation may need to have a wider dynamic range to handle both low and high concentrations.

The temporal resolution of radical measurements must be sufficiently short to capture changes in the concentrations of reactive species on the timescale of indoor activities such as cooking or cleaning. Real-time measurements with a measurement interval of a few minutes are adequate for many purposes. However, some of the techniques discussed above (such as derivatisation, followed by off-line analysis) have much longer sample acquisition times. Besides the extra effort and time required for off-line analysis, such approaches would be too slow to capture fast changes in indoor air composition and transformation.

The spatial variability of reactive species must also be evaluated. The high reactivity of some radical species and the location of different sources and sinks can produce significant variation in radical concentrations across an indoor space. It would therefore be advisable to compare fast radical measurements with integrated measurements (using for example, OH tracers). Comparative measurements in direct sunlight, and in the shade or dark zones, are needed to characterize and quantify the contribution of reactive chemistry in different locations in an indoor space. Such measurements would help to establish the relative importance of ozonolysis of alkenes versus photolytic sources, for example. The contribution of direct emissions (such as HONO from candles, gas fires, and stoves) is also unclear and could be extremely large; measurements around such sources are needed. This is an important question because the health impacts of combustion sources in confined indoor environments are of special concern, both from direct emissions and through their influence on indoor air chemistry.

In addition to chemical measurements, spatial differences in the actinic flux also influences the spatial variation in the concentrations and chemical processes taking place indoors. The transmission of light to the indoor environment affects HONO photolysis, to produce OH radicals, and other processes, such as chlorine chemistry and photosensitization processes mediated by several household chemicals. The actinic flux is therefore an important parameter in indoor photochemistry and should be measured at difference locations in an indoor space, in parallel with chemical observations. Measurements are also needed in a range of locations and conditions (including types of windows and building orientation) representative of the indoor environment.

Except for the Criegee intermediates and some chlorine species, techniques are now available which are sufficiently sensitive for exploring the contribution of radicals and their precursors to oxidation processes within the indoor environment. Previous studies of these species have already revealed surprises about their role in the indoor environment. However, comprehensive measurements of these species will not be routinely possible because monitoring atmospheric radicals and their precursors requires custom-built, highly specialized, and specific instrumentation. The most important exceptions in this regard are CIMS instruments (which can measure several of the above species, depending on the ionization source) and LOPAP (for HONO measurements). For other species requiring custom instruments, the instruments either have to be developed in-house — a formidable challenge — or measured in collaboration with research groups that possess the necessary instrumentation. In this case, the technique and instrument used will be dictated by instrument (and collaborator) availability. Nevertheless,

understanding indoor air chemistry is an important scientific objective, and some indoor air measurement campaigns will need to combine the instrumentation and collaborations needed to explore atmospheric chemistry in different indoor environments.

Continued improvement of existing techniques for outdoor measurements, and their adaptation for use in occupied indoor spaces, would also be beneficial. Sensitive and accurate measurements remain vital, as does extending measurements to other species of potential interest, like dicarbonylic products besides GLY and MGLY. Large radical campaigns including NO_y/VOC/radical/chlorine compound concentrations, actinic flux and the air exchange rate are also recommended.

To date, standardized measurement methods for the assessment of indoor air quality have been mainly based on discontinuous measurements of long-lived trace substances. The presence of short-lived indoor oxidants and their effect on the abundance of oxidation products that building occupants inhale, ingest or dermally absorb is not tackled by the internationally standardized assessment of indoor air quality. Future research efforts and corresponding standardization activities should focus on expanding our current understanding of the conditions and underlying chemistry that produce high concentrations of pollutants indoors.

Finally, complementary measurements of OH reactivity during standardized material emission tests can help to investigate potential uncertainties in material emissions with special regard to standardized test protocols and material labels. Such measurements will help derive estimates for the formation rate of secondary indoor pollutants resulting from OH-initiated oxidation processes.

Acknowledgements

This publication is based upon work from COST Action CA17136 - Indoor Air Pollution Network (INDAIRPOLLNET) supported by COST (European Cooperation in Science and Technology) (www.cost.eu) for which the authors are grateful. The assistance of Aime Ruus for formatting the manuscript is also warmly thanked.

Disclosure statement

No potential conflict of interest was reported by the authors.

ORCID

Elena Gómez Alvarez http://orcid.org/0000-0001-5235-9806
Viktor Gábor Mihucz http://orcid.org/0000-0002-5320-669X
Dean Venables http://orcid.org/0000-0002-4135-1793

References

1. Young, C. J.; Zhou, S.; Siegel, J. A.; Kahan, T. F. Illuminating the Dark Side of Indoor Oxidants. *Environ. Sci. Process Impacts* 2019, *21*, 1229–1239. doi:10.1039/c9em00111e
2. Gómez Alvarez, E.; Amedro, D.; Afif, C.; Gligorovski, S.; Schoemaecker, C.; Schoemacker, C.; Fittschen, C.; Doussin, J.-F.; Wortham, H. Unexpectedly High Indoor Hydroxyl Radical Concentrations Associated with Nitrous Acid. *Proc. Natl. Acad. Sci. U S A.* 2013, *110*, 13294–13299. doi:10.1073/pnas.1308310110

3. Brauer, M.; Ryan, P. B.; Suh, H. H.; Koutrakis, P.; Spengler, J. D.; Leslie, N. P.; Billick, I. H. Measurements of Nitrous Acid inside Two Research Houses. *Environ. Sci. Technol.* 1990, *24*, 1521–1527. doi:10.1021/es00080a011
4. Carslaw, N.; Fletcher, L.; Heard, D.; Ingham, T.; Walker, H. Significant OH Production under Surface Cleaning and Air Cleaning Conditions: Impact on Indoor Air Quality. *Indoor Air* 2017, *27*, 1091–1100. doi:10.1111/ina.12394
5. Arata, C.; Zarzana, K. J.; Misztal, P. K.; Liu, Y.; Brown, S. S.; Nazaroff, W. W.; Goldstein, A. H. Measurement of NO3 and N2O5 in a Residential Kitchen. *Environ. Sci. Technol. Lett* 2018, *5*, 595–599. doi:10.1021/ACS.ESTLETT.8B00415/SUPPL_FILE/EZ8B00415_SI_001.PDF
6. Wong, J. P. S.; Carslaw, N.; Zhao, R.; Zhou, S.; Abbatt, J. P. D. Observations and Impacts of Bleach Washing on Indoor Chlorine Chemistry. *Indoor Air* 2017, *27*, 1082–1090. doi:10.1111/ina.12402
7. Marciel Rosales, C. F.; Jiang, J.; Lahib, A.; Bottorff, B. P.; Reidy, E. K.; Kumar, V.; Tasoglou, A.; Huber, H.; Dusanter, S.; Tomas, A. Chemistry and Human Exposure Implications of Secondary Organic Aerosol Production from Indoor Terpene Ozonolysis. *Sci. Adv.* 2022, *8*.
8. Mattila, J. M.; Lakey, P. S. J.; Shiraiwa, M.; Wang, C.; Abbatt, J. P. D.; Arata, C.; Goldstein, A. H.; Ampollini, L.; Katz, E. F.; DeCarlo, P.; et al. Multiphase Chemistry Controls Inorganic Chlorinated and Nitrogenated Compounds in Indoor Air during Bleach Cleaning. *Environ. Sci. Technol* 2020, *54*, acs.est.1730–1739. doi:10.1021/acs.est.9b05767
9. Gandolfo, A.; Gligorovski, V.; Bartolomei, V.; Tlili, S.; Gómez Alvarez, E.; Wortham, H.; Kleffmann, J.; Gligorovski, S. Spectrally Resolved Actinic Flux and Photolysis Frequencies of Key Species within an Indoor Environment. *Build. Environ.* 2016, *109*, 50–57. doi:10.1016/j.buildenv.2016.08.026
10. Zhou, S.; Kowal, S. F.; Cregan, A. R.; Kahan, T. F. Factors Affecting Wavelength-Resolved Ultraviolet Irradiance Indoors and Their Impacts on Indoor Photochemistry. *Indoor Air* 2021, *31*, 1187–1198. doi:10.1111/ina.12784
11. Zhou, S.; Kahan, T. F. Spatiotemporal Characterization of Irradiance and Photolysis Rate Constants of Indoor Gas-Phase Species in the UTest House during HOMEChem. *Indoor Air* 2022, *32*, e12966. doi:10.1111/ina.12966
12. Stone, D.; Whalley, L. K.; Heard, D. E. Tropospheric OH and HO2 Radicals: Field Measurements and Model Comparisons. *Chem. Soc. Rev.* 2012, *41*, 6348. doi:10.1039/c2cs35140d
13. Dusanter, S.; Stevens, P. S. Recent Advances in the Chemistry of OH and HO_2 Radicals in the Atmosphere: Field and Laboratory Measurements. In *Advances in Atmospheric Chemistry; Advances in Atmospheric Chemistry*; World Scientific Publishing Company Incorporated, 2017; Vol. 1, p 493–579. 10.1142/9789813147355_0007.
14. Heard, D. E.; Pilling, M. J. Measurement of OH and HO2 in the Troposphere. *Chem. Rev.* 2003, *103*, 5163–5198. doi:10.1021/cr020522s
15. Faloona, I. C.; Tan, D.; Lesher, R. L.; Hazen, N. L.; Frame, C. L.; Simpas, J. B.; Harder, H.; Martinez, M.; Di Carlo, P.; Ren, X.; Brune, W. H. A Laser-Induced Fluorescence Instrument for Detecting Tropospheric OH and HO2: Characteristics and Calibration. *J. Atmos. Chem.* 2004, *47*, 139–167. doi:10.1023/B:JOCH.0000021036.53185.0e
16. Dorn, H. P.; Neuroth, R.; Hofzumahaus, A. Investigation of OH Absorption Cross Sections of Rotational Transitions in the $A2\Sigma+$, $V'=0 \leftarrow X2\Pi$, $V''=0$ Band under Atmospheric Conditions: Implications for Tropospheric Long-Path Absorption Measurements. *J. Geophys. Res.* 1995, *100*, 7397–7409. doi:10.1029/94JD03323
17. Mercier, X.; Therssen, E.; Pauwels, J. F.; Desgroux, P. Cavity Ring-down Measurements of OH Radical in Atmospheric Premixed and Diffusion Flames.: a Comparison with Laser-Induced Fluorescence and Direct Laser Absorption. *Chem. Phys. Lett.* 1999, *299*, 75–83. doi:10.1016/S0009-2614(98)01233-0

18. Meyer, T. R.; Roy, S.; Anderson, T. N.; Miller, J. D.; Katta, V. R.; Lucht, R. P.; Gord, J. R. Measurements of OH Mole Fraction and Temperature up to 20 KHz by Using a Diode-Laser-Based UV Absorption Sensor. *Appl. Opt.* 2005, *44*, 6729–6740. doi:10.1364/AO.44.006729
19. Guoli, Z.; Aimin, Z.; Jiating, W.; Zhongwei, L.; Yong, X. Measurement of OH Radicals in Dielectric Barrier Discharge Plasmas by Cavity Ring-Down Spectroscopy. *Plasma Sci. Technol.* 2010, *12*, 166–171. doi:10.1088/1009-0630/12/2/08
20. Assaf, E.; Fittschen, C. Cross Section of OH Radical Overtone Transition near 7028 cm(-1) and Measurement of the Rate Constant of the Reaction of OH with HO2 Radicals. *J. Phys. Chem. A.* 2016, *120*, 7051–7059. doi:10.1021/acs.jpca.6b06477
21. Peeters, R.; Berden, G.; Ólafsson, A.; Laarhoven, L. J. J.; Meijer, G. Cavity Enhanced Absorption Spectroscopy in the 10 Mm Region Using a Waveguide CO2 Laser. *Chem. Phys. Lett* 2001, *337*, 231–236. doi:10.1016/S0009-2614(01)00217-2
22. Aizawa, T. Diode-Laser Wavelength-Modulation Absorption Spectroscopy for Quantitative in Situ Measurements of Temperature and OH Radical Concentration in Combustion Gases. *Appl. Opt.* 2001, *40*, 4894–4903. doi:10.1364/ao.40.004894
23. Blitz, M. A.; Salter, R. J.; Heard, D. E.; Seakins, P. W. An Experimental Study of the Kinetics of OH/OD(v = 1,2,3) + SO2: The Limiting High-Pressure Rate Coefficients as a Function of Temperature. *J. Phys. Chem. A.* 2017, *121*, 3175–3183. doi:10.1021/acs.jpca.7b01294
24. Pesce, G.; Rusciano, G.; Sasso, A. Detection and Spectroscopy of OH Fundamental Vibrational Band Based on a Difference Frequency Generator at 3 Mm. *Chem. Phys. Lett* 2003, *374*, 425–431. doi:10.1016/S0009-2614(03)00528-1
25. Zhao, W.; Wysocki, G.; Chen, W.; Fertein, E.; Le Coq, D.; Petitprez, D.; Zhang, W. Sensitive and Selective Detection of OH Radicals Using Faraday Rotation Spectroscopy at 2.8 Mm. *Opt. Express* 2011, *19*, 2493–2501. doi:10.1364/OE.19.002493
26. Tanner, D. J.; Jefferson, A.; Eisele, F. L. Selected Ion Chemical Ionization Mass Spectrometric Measurement of OH. *J. Geophys. Res.* 1997, *102*, 6415–6425. doi:10.1029/96JD03919
27. Smith, S. C.; Lee, J. D.; Bloss, W. J.; Johnson, G. P.; Ingham, T.; Heard, D. E. Concentrations of OH and HO≪Sub≫2≪/Sub≫ Radicals during NAMBLEX: Measurements and Steady State Analysis. *Atmos. Chem. Phys* 2006, *6*, 1435–1453. doi:10.5194/acp-6-1435-2006
28. Novelli, A.; Hens, K.; Tatum Ernest, C.; Kubistin, D.; Regelin, E.; Elste, T.; Plass-Dülmer, C.; Martinez, M.; Lelieveld, J.; Harder, H. Characterisation of an Inlet Pre-Injector Laser-Induced Fluorescence Instrument for the Measurement of Atmospheric Hydroxyl Radicals. *Atmos. Meas. Tech* 2014, *7*, 3413–3430. doi:10.5194/amt-7-3413-2014
29. Holland, F.; Hessling, M.; Hofzumahaus, A. In Situ Measurement of Tropospheric OH Radicals by Laser-Induced Fluorescence—a Description of the KFA Instrument. *J. Atmos. Sci.* 1995, *52*, 3393–3401. doi:10.1175/1520-0469(1995)052 < 3393:ISMOTO > 2.0.CO;2
30. Dusanter, S.; Vimal, D.; Stevens, P. S.; Volkamer, R.; Molina, L. T. Measurements of OH and HO2 Concentrations during the MCMA-2006 Field Campaign – Part 1: Deployment of the Indiana University Laser-Induced Fluorescence Instrument. *Atmos. Chem. Phys* 2009, *9*, 1665–1685. doi:10.5194/acp-9-1665-2009
31. Amedro, D. *Atmospheric Measurements of OH and HO2 Radicals Using FAGE: Development and Deployment on the Field*; University of Lille, 2012.
32. Tan, Z.; Fuchs, H.; Lu, K.; Hofzumahaus, A.; Bohn, B.; Broch, S.; Dong, H.; Gomm, S.; Häseler, R.; He, L.; et al. Radical Chemistry at a Rural Site (Wangdu) in the North China Plain: Observation and Model Calculations of\Chem{OH},\Chem{HO_2} and\Chem{RO_2} Radicals. *Atmos. Chem. Phys* 2017, *17*, 663–690. doi:10.5194/acp-17-663-2017
33. Wang, F.; Hu, R.; Chen, H.; Xie, P.; Wang, Y.; Li, Z.; Jin, H.; Liu, J.; Liu, W. Development of a Field System for Measurement of Tropospheric OH Radical Using Laser-Induced Fluorescence Technique. *Opt Express* 2019, *27*, A419–A435. doi:10.1364/OE.27.00A419

34. Mao, J.; Ren, X.; Zhang, L.; Van Duin, D. M.; Cohen, R. C.; Park, J.-H.; Goldstein, A. H.; Paulot, F.; Beaver, M. R.; Crounse, J. D.; et al. Insights into Hydroxyl Measurements and Atmospheric Oxidation in a California Forest. *Atmos. Chem. Phys* 2012, *12*, 8009–8020. doi:10.5194/acp-12-8009-2012
35. Woodward-Massey, R.; Slater, E. J.; Alen, J.; Ingham, T.; Cryer, D. R.; Stimpson, L. M.; Ye, C.; Seakins, P. W.; Whalley, L. K.; Heard, D. E. Implementation of a Chemical Background Method for Atmospheric OH Measurements by Laser-Induced Fluorescence: Characterisation and Observations from the UK and China. *Atmos. Meas. Tech.* 2020, *13*, 3119–3146. doi:10.5194/amt-13-3119-2020
36. Cho, C.; Hofzumahaus, A.; Fuchs, H.; Dorn, H.-P.; Glowania, M.; Holland, F.; Rohrer, F.; Vardhan, V.; Kiendler-Scharr, A.; Wahner, A.; et al. Characterization of a Chemical Modulation Reactor (CMR) for the Measurement of Atmospheric Concentrations of Hydroxyl Radicals with a Laser-Induced Fluorescence Instrument. *Atmos. Meas. Tech.* 2021, *14*, 1851–1877. doi:10.5194/amt-14-1851-2021
37. Mauldin, R. L.; Kosciuch, E.; Henry, B. E.; Eisele, F.; Shetter, R.; Lefer, B.; Chen, G.; Davis, D.; Huey, G.; Tanner, D. Measurements of OH, HO2+ RO2, H2SO4, and MSA at the South Pole during ISCAT 2000. *Atmos. Environ.* 2004, *38*, 5423–5437. doi:10.1016/j.atmosenv.2004.06.031
38. Aufmhoff, H.; Hanke, M.; Uecker, J.; Schlager, H.; Arnold, F. An Ion Trap CIMS Instrument for Combined Measurements of Atmospheric OH and H2SO4: First Test Measurements above and inside the Planetary Boundary Layer. *Int. J. Mass Spectrom* 2011, *308*, 26–34. doi:10.1016/j.ijms.2011.07.016
39. Kukui, A.; Ancellet, G.; Le Bras, G. Chemical Ionisation Mass Spectrometer for Measurements of OH and Peroxy Radical Concentrations in Moderately Polluted Atmospheres. *J Atmos Chem* 2008, *61*, 133–154. doi:10.1007/s10874-009-9130-9
40. Hausmann, M.; Brandenburger, U.; Brauers, T.; Dorn, H.-P. Detection of Tropospheric OH Radicals by Long-Path Differential-Optical-Absorption Spectroscopy: Experimental Setup, Accuracy, and Precision. *J. Geophys. Res* 1997, *102*, 16011–16022. doi:10.1029/97JD00931
41. Fuchs, H.; Dorn, H.-P.; Bachner, M.; Bohn, B.; Brauers, T.; Gomm, S.; Hofzumahaus, A.; Holland, F.; Nehr, S.; Rohrer, F.; et al. Comparison of OH Concentration Measurements by DOAS and LIF during SAPHIR Chamber Experiments at High OH Reactivity and Low NO Concentration. *Atmos. Meas. Tech* 2012, *5*, 1611–1626. doi:10.5194/amt-5-1611-2012
42. Kovacs, T. A.; Brune, W. H. Total OH Loss Rate Measurement. *J. Atmos. Chem* 2001, *39*, 105–122. doi:10.1023/A:1010614113786
43. Sadanaga, Y.; Yoshino, A.; Watanabe, K.; Yoshioka, A.; Wakazono, Y.; Kanaya, Y.; Kajii, Y. Development of a Measurement System of OH Reactivity in the Atmosphere by Using a Laser-Induced Pump and Probe Technique. *Rev. Sci. Instrum* 2004, *75*, 2648–2655. doi:10.1063/1.1775311
44. Muller, J. B. A.; Elste, T.; Plass-Dülmer, C.; Stange, G.; Holla, R.; Claude, A.; Englert, J.; Gilge, S.; Kubistin, D. A Novel Semi-Direct Method to Measure\Chem{OH} Reactivity by Chemical Ionization Mass Spectrometry (CIMS). *Atmos. Meas. Tech.* 2018, *11*, 4413–4433. doi:10.5194/amt-11-4413-2018
45. Fuchs, H.; Novelli, A.; Rolletter, M.; Hofzumahaus, A.; Pfannerstill, E. Y.; Kessel, S.; Edtbauer, A.; Williams, J.; Michoud, V.; Dusanter, S.; et al. Comparison of OH Reactivity Measurements in the Atmospheric Simulation Chamber SAPHIR. *Atmos. Meas. Tech* 2017, *10*, 4023–4053. doi:10.5194/amt-10-4023-2017
46. Michoud, V.; Hansen, R. F.; Locoge, N.; Stevens, P. S.; Dusanter, S. Detailed Characterizations of the New Mines Douai Comparative Reactivity Method Instrument via Laboratory Experiments and Modeling. *Atmos. Meas. Tech.* 2015, *8*, 3537–3553. doi:10.5194/amt-8-3537-2015
47. Zannoni, N.; Dusanter, S.; Gros, V.; Sarda Esteve, R.; Michoud, V.; Sinha, V.; Locoge, N.; Bonsang, B. Intercomparison of Two Comparative Reactivity Method Instruments Inf the

Mediterranean Basin during Summer 2013. *Atmos. Meas. Tech* 2015, *8*, 3851–3865. doi:10.5194/amt-8-3851-2015

48. Sinha, V.; Williams, J.; Crowley, J. N.; Lelieveld, J. The Comparative Reactivity Method &Ndash; a New Tool to Measure Total OH Reactivity in Ambient Air. *Atmos. Chem. Phys.* 2008, *8*, 2213–2227. doi:10.5194/acp-8-2213-2008
49. Mao, J.; Ren, X.; Brune, W. H.; Olson, J. R.; Crawford, J. H.; Fried, A.; Huey, L. G.; Cohen, R. C.; Heikes, B.; Singh, H. B.; et al. Airborne Measurement of OH Reactivity during INTEX-B. *Atmos. Chem. Phys.* 2009, *9*, 163–173. doi:10.5194/acp-9-163-2009
50. Parker, A. E.; Amédro, D.; Schoemaecker, C.; Fittschen, C. OH Radical Reactivity Measurements by FAGE. *Environ. Eng. Manag. J.* 2011, *10*, 107–114. doi:10.30638/eemj.2011.015
51. Stone, D.; Whalley, L. K.; Ingham, T.; Edwards, P. M.; Cryer, D. R.; Brumby, C. A.; Seakins, P. W.; Heard, D. E. Measurement of OH Reactivity by Laser Flash Photolysis Coupled with Laser-Induced Fluorescence Spectroscopy. *Atmos. Meas. Tech.* 2016, *9*, 2827–2844. doi:10.5194/amt-9-2827-2016
52. Lou, S.; Holland, F.; Rohrer, F.; Lu, K.; Bohn, B.; Brauers, T.; Chang, C. C.; Fuchs, H.; Häseler, R.; Kita, K.; et al. Atmospheric OH Reactivities in the Pearl River Delta – China in Summer 2006: Measurement and Model Results. *Atmos. Chem. Phys.* 2010, *10*, 11243–11260. doi:10.5194/acp-10-11243-2010
53. Fuchs, H.; Tan, Z.; Hofzumahaus, A.; Broch, S.; Dorn, H.-P.; Holland, F.; Künstler, C.; Gomm, S.; Rohrer, F.; Schrade, S.; et al. Investigation of Potential Interferences in the Detection of Atmospheric RO$_x$Radicals by Laser-Induced Fluorescence\Hack{\Break} under Dark Conditions. *Atmos. Meas. Tech.* 2016, *9*, 1431–1447. doi:10.5194/amt-9-1431-2016
54. Berresheim, H.; Elste, T.; Plass-Dülmer, C.; Eiseleb, F. L.; Tannerb, D. J. Chemical Ionization Mass Spectrometer for Long-Term Measurements of Atmospheric OH and H2SO4. *Int. J. Mass Spectrom* 2000, *202*, 91–109. doi:10.1016/S1387-3806(00)00233-5
55. Fuchs, H.; Bohn, B.; Hofzumahaus, A.; Holland, F.; Lu, K. D.; Nehr, S.; Rohrer, F.; Wahner, A. Detection of HO2 by Laser-Induced Fluorescence: Calibration and Interferences from RO2 Radicals. *Atmos. Meas. Tech.* 2011, *4*, 1209–1225. doi:10.5194/amt-4-1209-2011
56. Whalley, L. K.; Blitz, M. A.; Desservettaz, M.; Seakins, P. W.; Heard, D. E. Reporting the Sensitivity of Laser-Induced Fluorescence Instruments Used for HO2 Detection to an Interference from RO2 Radicals and Introducing a Novel Approach That Enables HO2 and Certain RO2 Types to Be Selectively Measured. *Atmos. Meas. Tech.* 2013, *6*, 3425–3440. doi:10.5194/amt-6-3425-2013
57. Wang, Y.; Hu, R.; Xie, P.; Chen, H.; Wang, F.; Liu, X.; Liu, J.; Liu, W. Measurement of Tropospheric HO2 Radical Using Fluorescence Assay by Gas Expansion with Low Interferences. *J. Environ. Sci. (China)* 2021, *99*, 40–50. doi:10.1016/j.jes.2020.06.010
58. Hanke, M.; Uecker, J.; Reiner, T.; Arnold, F. Atmospheric Peroxy Radicals: ROXMAS, a New Mass-Spectrometric Methodology for Speciated Measurements of HO2 and $\sum$RO2 and First Results. *Int. J. Mass Spectrom.* 2002, *213*, 91–99. doi:10.1016/S1387-3806(01)00548-6
59. Edwards, G. D.; Cantrell, C. A.; Stephens, S.; Hill, B.; Goyea, O.; Shetter, R. E.; Mauldin, R. L.; Kosciuch, E.; Tanner, D. J.; Eisele, F. L. Chemical Ionization Mass Spectrometer Instrument for the Measurement of Tropospheric HO2 and RO2. *Anal. Chem.* 2003, *75*, 5317–5327. doi:10.1021/ac034402b
60. Wolfe, G. M.; Cantrell, C.; Kim, S.; Mauldin, R. L.; III, Karl, T.; Harley, P.; Turnipseed, A.; Zheng, W.; Flocke, F.; Apel, E. C.; et al. Missing Peroxy Radical Sources within a Summertime Ponderosa Pine Forest. *Atmos. Chem. Phys* 2014, *14*, 4715–4732. doi:10.5194/acp-14-4715-2014
61. Miyazaki, K.; Parker, A. E.; Fittschen, C.; Monks, P. S.; Kajii, Y. A New Technique for the Selective Measurement of Atmospheric Peroxy Radical Concentrations of HO$_{2}$and

RO$_{2}$Using a Denuding Method. *Atmos. Meas. Tech* 2010, *3*, 1547–1554. doi:10.5194/amt-3-1547-2010

62. Sanchez, J.; Tanner, D. J.; Chen, D.; Huey, L. G.; Ng, N. L. A New Technique for the Direct Detection of HO2 Radicals Using Bromide Chemical Ionization Mass Spectrometry (Br-CIMS): Initial Characterization. *Atmos. Meas. Tech.* 2016, *9*, 3851–3861. doi:10.5194/amt-9-3851-2016
63. Albrecht, S. R.; Novelli, A.; Hofzumahaus, A.; Kang, S.; Baker, Y.; Mentel, T.; Wahner, A.; Fuchs, H. Measurements of Hydroperoxy Radicals (HO2) at Atmospheric Concentrations Using Bromide Chemical Ionisation Mass Spectrometry. *Atmos. Meas. Tech.* 2019, *12*, 891–902. doi:10.5194/amt-12-891-2019
64. Hong, Z.; Davidson, D. F.; Lam, K.-Y.; Hanson, R. K. A Shock Tube Study of the Rate Constants of HO2 and CH3 Reactions. *Combust. Flame* 2012, *159*, 3007–3013. doi:10.1016/j.combustflame.2012.04.009
65. Tomas, A.; Villenave, E.; Lesclaux, R. Reactions of the HO2 Radical with CH3CHO and CH3C(O)O2 in the Gas Phase. *J. Phys. Chem. A.* 2001, *105*, 3505–3514. doi:10.1021/jp003762p
66. Christensen, L. E.; Okumura, M.; Sander, S. P.; Friedl, R. R.; Miller, C. E.; Sloan, J. J. Measurements of the Rate Constant of HO2 + NO2 + N2 → HO2NO2 + N2 Using near-Infrared Wavelength-Modulation Spectroscopy and UV − Visible Absorption Spectroscopy. *J. Phys. Chem. A.* 2004, *108*, 80–91. doi:10.1021/jp035905o
67. Thiébaud, J.; Fittschen, C. Near Infrared Cw-CRDS Coupled to Laser Photolysis: Spectroscopy and Kinetics of the HO2 Radical. *Appl. Phys. B.* 2006, *85*, 383–389. doi:10.1007/s00340-006-2304-0
68. Gianella, M.; Reuter, S.; Aguila, A. L.; Ritchie, G. A. D.; Helden, J-PHv. Detection of HO2in an Atmospheric Pressure Plasma Jet Using Optical Feedback Cavity-Enhanced Absorption Spectroscopy. *New J. Phys.* 2016, *18*, 113027. doi:10.1088/1367-2630/18/11/113027
69. Bell, C. L.; van Helden, J.-P. H.; Blaikie, T. P. J.; Hancock, G.; van Leeuwen, N. J.; Peverall, R.; Ritchie, G. A. D. Noise-Immune Cavity-Enhanced Optical Heterodyne Detection of HO2 in the near-Infrared Range. *J. Phys. Chem. A.* 2012, *116*, 5090–5099. doi:10.1021/jp301038r
70. Brumfield, B.; Sun, W.; Ju, Y.; Wysocki, G. Direct in Situ Quantification of HO2 from a Flow Reactor. *J. Phys. Chem. Lett.* 2013, *4*, 872–876. doi:10.1021/jz400143c
71. Onel, L.; Brennan, A.; Seakins, P. W.; Whalley, L.; Heard, D. E. A New Method for Atmospheric Detection of the CH3O2 Radical. *Atmos. Meas. Tech.* 2017, *10*, 3985–4000. doi:10.5194/amt-10-3985-2017
72. Onel, L.; Brennan, A.; Gianella, M.; Hooper, J.; Ng, N.; Hancock, G.; Whalley, L.; Seakins, P. W.; Ritchie, G. A. D.; Heard, D. E. An Intercomparison of CH3O2 Measurements by Fluorescence Assay by Gas Expansion and Cavity Ring-down Spectroscopy within HIRAC (Highly Instrumented Reactor for Atmospheric Chemistry). *Atmos. Meas. Tech.* 2020, *13*, 2441–2456. doi:10.5194/amt-13-2441-2020
73. Whalley, L. K.; Stone, D.; Dunmore, R.; Hamilton, J.; Hopkins, J. R.; Lee, J. D.; Lewis, A. C.; Williams, P.; Kleffmann, J.; Laufs, S.; et al. Understanding in Situ Ozone Production in the Summertime through Radical Observations and Modelling Studies during the Clean Air for London Project (ClearfLo). *Atmos. Chem. Phys.* 2018, *18*, 2547–2571. doi:10.5194/acp-18-2547-2018
74. Fuchs, H.; Holland, F.; Hofzumahaus, A. Measurement of Tropospheric R O2 and HO2 Radicals by a Laser-Induced Fluorescence Instrument. *Rev. Sci. Instrum.* 2008, *79*, 1–12. doi:10.1063/1.2968712
75. Hornbrook, R. S.; Crawford, J. H.; Edwards, G. D.; Goyea, O.; Mauldin, R. L.; III, Olson, J. S.; Cantrell, C. A. Measurements of Tropospheric HO2 and RO2 by Oxygen Dilution Modulation and Chemical Ionization Mass Spectrometry. *Atmos. Meas. Tech* 2011, *4*, 735–756. doi:10.5194/amt-4-735-2011

76. Parker, A. E.; Monks, P. S.; Wyche, K. P.; Balzani-Lööv, J. M.; Staehelin, J.; Reimann, S.; Legreid, G.; Vollmer, M. K.; Steinbacher, M. Peroxy Radicals in the Summer Free Troposphere: Seasonality and Potential for Heterogeneous Loss. *Atmos. Chem. Phys* 2009, *9*, 1989–2006. doi:10.5194/acp-9-1989-2009
77. Liu, Y.; Morales-Cueto, R.; Hargrove, J.; Medina, D.; Zhang, J. Measurements of Peroxy Radicals Using Chemical Amplification-Cavity Ringdown Spectroscopy. *Environ. Sci. Technol.* 2009, *43*, 7791–7796. doi:10.1021/es901146t
78. Wood, E. C.; Charest, J. R. Chemical Amplification-Cavity Attenuated Phase Shift Spectroscopy Measurements of Atmospheric Peroxy Radicals. *Anal Chem* 2014, *86*, 10266–10273. doi:10.1021/ac502451m
79. Lahib, A. *Analytical Developments for Measuring Atmospheric Peroxy Radicals*; University of Lille, 2019.
80. Duncianu, M.; Lahib, A.; Tomas, A.; Stevens, P. S.; Dusanter, S. Characterization of a Chemical Amplifier for Peroxy Radical Measurements in the Atmosphere. *Atmos. Environ* 2020, *222*, 117106. doi:10.1016/j.atmosenv.2019.117106
81. English, A. M.; Hansen, J. C.; Szente, J. J.; Maricq, M. M. The Effects of Water Vapor on the CH3O2 Self-Reaction and Reaction with HO2. *J. Phys. Chem. A.* 2008, *112*, 9220–9228. doi:10.1021/jp800727a
82. Faragó, E. P.; Viskolcz, B.; Schoemaecker, C.; Fittschen, C. Absorption Spectrum and Absolute Absorption Cross Sections of CH3O2 Radicals and CH3I Molecules in the Wavelength Range 7473-7497 cm(-1). *J. Phys. Chem. A.* 2013, *117*, 12802–12811. doi:10.1021/jp408686s
83. Meloni, G.; Zou, P.; Klippenstein, S. J.; Ahmed, M.; Leone, S. R.; Taatjes, C. A.; Osborn, D. L. Energy-Resolved Photoionization of Alkylperoxy Radicals and the Stability of Their Cations. *J. Am. Chem. Soc.* 2006, *128*, 13559–13567. doi:10.1021/ja064556j
84. Berndt, T.; Scholz, W.; Mentler, B.; Fischer, L.; Herrmann, H.; Kulmala, M.; Hansel, A. Accretion Product Formation from Self- and Cross-Reactions of RO2 Radicals in the Atmosphere. *Angew. Chem. Int. Ed.* 2018, *57*, 3820–3824. doi:10.1002/anie.201710989
85. Pitts, J. N.; Grosjean, D.; Van Cauwenberghe, K.; Schmid, J.; Fitz, D. Photooxidation of Aliphatic Amines under Simulated Atmospheric Conditions: Formation of Nitrosamines, Nitramines, Amides, and Photochemical Oxidant. *Environ. Sci. Technol.* 1978, *12*, 946–953. doi:10.1021/es60144a009
86. Sleiman, M.; Gundel, L. A.; Pankow, J. F.; Jacob, P.; Singer, B. C.; Destaillats, H. Formation of Carcinogens Indoors by Surface-Mediated Reactions of Nicotine with Nitrous Acid, Leading to Potential Thirdhand Smoke Hazards. *Proc. Natl. Acad. Sci. U S A.* 2010, *107*, 6576–6581. doi:10.1073/pnas.0912820107
87. Grassian, V. H. Heterogeneous Uptake and Reaction of Nitrogen Oxides and Volatile Organic Compounds on the Surface of Atmospheric Particles Including Oxides, Carbonates, Soot and Mineral Dust: Implications for the Chemical Balance of the Troposphere. *Int. Rev. Phys. Chem.* 2001, *20*, 467–548. doi:10.1080/01442350110051968
88. Finlayson-Pitts, B. J.; Wingen, L. M.; Sumner, A. L.; Syomin, D.; Ramazan, K. A. The Heterogeneous Hydrolysis of NO2 in Laboratory Systems and in Outdoor and Indoor Atmospheres: An Integrated Mechanism. *Phys. Chem. Chem. Phys.* 2003, *5*, 223–242. doi:10.1039/b208564j
89. Ammann, M.; Rössler, E.; Strekowski, R.; George, C. Nitrogen Dioxide Multiphase Chemistry: Uptake Kinetics on Aqueous Solutions Containing Phenolic Compounds. *Phys. Chem. Chem. Phys.* 2005, *7*, 2513–2518. doi:10.1039/b501808k
90. George, C.; Strekowski, R. S.; Kleffmann, J.; Stemmler, K.; Ammann, M. Photoenhanced Uptake of Gaseous NO2 on Solid Organic Compounds: A Photochemical Source of HONO? *Faraday Discuss* 2005, *130*, 195–210. doi:10.1039/b417888m
91. Santis, F.; Montagnoli, M.; Pasella, D.; Allegrini, I. The Measurement and Model Predictions of Photochemical Pollutants in the Uffizi Gallery. *Florence. Ann. Chim* 1999, *89*, 679–688.

92. Leaderer, B. P.; Naeher, L.; Jankun, T.; Balenger, K.; Holford, T. R.; Toth, C.; Sullivan, J.; Wolfson, J. M.; Koutrakis, P. Indoor, Outdoor, and Regional Summer and Winter Concentrations of PM10, PM2.5, SO4(2)-, H+, NH4+, NO3-, NH3, and Nitrous Acid in Homes with and without Kerosene Space Heaters. *Environ. Health Perspect.* 1999, *107*, 223–231. doi:10.1289/ehp.99107223
93. Lee, K.; Xue, J.; Geyh, A. S.; Özkaynak, H.; Leaderer, B. P.; Weschler, C. J.; Spengler, J. D. Nitrous Acid, Nitrogen Dioxide, and Ozone Concentrations in Residential Environments. *Environ. Health Perspect.* 2002, *110*, 145–149. doi:10.1289/ehp.02110145
94. Khoder, M. I. Nitrous Acid Concentrations in Homes and Offices in Residential Areas in Greater Cairo. *J. Environ. Monit.* 2002, *4*, 573–578. doi:10.1039/b201818g
95. Vichi, F.; Mašková, L.; Frattoni, M.; Imperiali, A.; Smolík, J. Simultaneous Measurement of Nitrous acid, nitric Acid, and Nitrogen Dioxide by Means of a Novel Multipollutant Diffusive Sampler in Libraries and Archives. *Herit. Sci.* 2016, *4*, 4. doi:10.1186/s40494-016-0074-5
96. Zhou, S.; Young, C. J.; Vandenboer, T. C.; Kowal, S. F.; Kahan, T. F. Time-Resolved Measurements of Nitric Oxide, Nitrogen Dioxide, and Nitrous Acid in an Occupied New York Home. *Environ. Sci. Technol.* 2018, *52*, 8355–8364. doi:10.1021/acs.est.8b01792
97. Collins, D. B.; Hems, R. F.; Zhou, S.; Wang, C.; Grignon, E.; Alavy, M.; Siegel, J. A.; Abbatt, J. P. D. Evidence for Gas-Surface Equilibrium Control of Indoor Nitrous Acid. *Environ. Sci. Technol.* 2018, *52*, 12419–12427. doi:10.1021/acs.est.8b04512
98. Pttts, J. N.; Wallington, T. J.; Biermann, H. W.; Winer, A. M. Identification and Measurement of Nitrous Acid in an Indoor Environment. *Atmos. Environ.* 1985, *19*, 763–767. doi:10.1016/0004-6981(85)90064-2
99. Salmon, L. G.; Nazaroff, W. W.; Ligocki, M. P.; Jones, M. C.; Cass, G. R. Nitric Acid Concentrations in Southern California Museums. *Environ. Sci. Technol.* 1990, *24*, 1004–1013. doi:10.1021/es00077a009
100. De Santis, F.; Di Palo, V.; Allegrini, I. Determination of Some Atmospheric Pollutants inside a Museum: Relationship with the Concentration Outside. *Sci. Total Environ.* 1992, *127*, 211–223. doi:10.1016/0048-9697(92)90504-L
101. Vecera, Z.; Dasgupta, P. Measurement of Atmospheric Nitric and Nitrous Acids with a Wet Effluent Diffusion Denuder and Low-Pressure Ion Chromatography-Postcolumn Reaction Detection. *Anal. Chem.* 1991, *63*, 2210–2216. doi:10.1021/ac00020a003
102. Spengler, J.; Brauer, M.; Samet, J.; Lambert, W. Nitrous Acid in Albuquerque, New Mexico, Homes. *Environ. Sci. Technol.* 1993, *27*, 841–845. doi:10.1021/es00042a005
103. Spicer, C. W.; Kenny, D. V.; Ward, G. F.; Billick, I. H. Transformations, Lifetimes, and Sources of NO2, HONO, and HNO3 in Indoor Environments. *Air Waste* 1993, *43*, 1479–1485. doi:10.1080/1073161x.1993.10467221
104. Vecera, Z.; Dasgupta, P. K. Indoor Nitrous Acid Levels. Production of Nitrous Acid from Open-Flame Sources. *Int. J. Environ. Anal. Chem.* 1994, *56*, 311–316. doi:10.1080/03067319408034109
105. Allen, A. G.; Miguel, A. H. Indoor Organic and Inorganic Pollutants: In-Situ Formation and Dry Deposition in Southeastern Brazil. *Atmos. Environ.* 1995, *29*, 3519–3526. doi:10.1016/1352-2310(95)00172-U
106. Simon, P. K.; Dasgupta, P. K. Continuous Automated Measurement of Gaseous Nitrous and Nitric Acids and Particulate Nitrite and Nitrate. *Environ. Sci. Technol.* 1995, *29*, 1534–1541.
107. Febo, A.; Perrino, C. Prediction and Experimental Evidence for High Air Concentration of Nitrous Acid in Indoor Environments. *Atmos. Environ. Part A. Gen. Top.* 1991, *25*, 1055–1061. doi:10.1016/0960-1686(91)90147-Y
108. Dunlea, E. J.; Herndon, S. C.; Nelson, D. D.; Volkamer, R. M.; San Martini, F.; Sheehy, P. M.; Zahniser, M. S.; Shorter, J. H.; Wormhoudt, J. C.; Lamb, B. K. Evaluation of Nitrogen Dioxide Chemiluminescence Monitors in a Polluted Urban Environment. *Atmos. Chem. Phys. Discuss* 2007, *7*, 569–604. doi:10.5194/acpd-7-569-2007

109. Villena, G.; Bejan, I.; Kurtenbach, R.; Wiesen, P.; Kleffmann, J. Interferences of Commercial NO2 Instruments in the Urban Atmosphere and in a Smog Chamber. *Atmos. Meas. Tech* 2012, *5*, 149–159. doi:10.5194/amt-5-149-2012
110. Gherman, T.; Venables, D. S.; Vaughan, S.; Orphal, J.; Ruth, A. A. Incoherent Broadband Cavity-Enhanced Absorption Spectroscopy in the near-Ultraviolet: Application to HONO and NO2. *Environ. Sci. Technol.* 2008, *42*, 890–895. doi:10.1021/es0716913
111. Duan, J.; Qin, M.; Ouyang, B.; Fang, W.; Li, X.; Lu, K.; Tang, K.; Liang, S.; Meng, F.; Hu, Z.; et al. Development of an Incoherent Broadband Cavity-Enhanced Absorption Spectrometer for in Situ Measurements\Hack{\Break}of HONO and\Chem{NO_2}. *Atmos. Meas. Tech* 2018, *11*, 4531–4543. doi:10.5194/amt-11-4531-2018
112. Bottorff, B.; Reidy, E.; Mielke, L.; Dusanter, S.; Stevens, P. S. Development of a Laser-Photofragmentation Laser-Induced Fluorescence Instrument for the Detection of Nitrous Acid and Hydroxyl Radicals in the Atmosphere. *Atmos. Meas. Tech* 2021, *14*, 6039–6056. doi:10.5194/amt-14-6039-2021
113. Jurkat, T.; Voigt, C.; Arnold, F.; Schlager, H.; Kleffmann, J.; Aufmhoff, H.; Schäuble, D.; Schaefer, M.; Schumann, U. Measurements of HONO, NO, NOy and SO2 in Aircraft Exhaust Plumes at Cruise. *Geophys. Res. Lett* 2011, *38*, n/a–5. doi:10.1029/2011GL046884
114. Bartolomei, V.; Gomez Alvarez, E.; Wittmer, J.; Tlili, S.; Strekowski, R.; Temime-Roussel, B.; Quivet, E.; Wortham, H.; Zetzsch, C.; Kleffmann, J.; Gligorovski, S. Combustion Processes as a Source of High Levels of Indoor Hydroxyl Radicals (OH) through the Photolysis of Nitrous Acid (HONO). *Environ. Sci. Technol.* 2015, *49*, 6599–6607. doi:10.1021/acs.est.5b01905
115. Gandolfo, A.; Bartolomei, V.; Gomez Alvarez, E.; Tlili, S.; Gligorovski, S.; Kleffmann, J.; Wortham, H. The Effectiveness of Indoor Photocatalytic Paints on NOx and HONO Levels. *Appl. Catal. B Environ* 2015, *166-167*, 84–90. doi:10.1016/j.apcatb.2014.11.011
116. Liu, J.; Li, S.; Zeng, J.; Mekic, M.; Yu, Z.; Zhou, W.; Loisel, G.; Gandolfo, A.; Song, W.; Wang, X.; et al. Assessing Indoor Gas Phase Oxidation Capacity through Real-Time Measurements of HONO and NOx in Guangzhou, China. *Environ. Sci. Process Impacts* 2019, *21*, 1393–1402. doi:10.1039/c9em00194h
117. Liu, J.; Deng, H.; Lakey, P. S. J.; Jiang, H.; Mekic, M.; Wang, X.; Shiraiwa, M.; Gligorovski, S. Unexpectedly High Indoor HONO Concentrations Associated with Photochemical NO2 Transformation on Glass Windows. *Environ. Sci. Technol.* 2020, *54*, 15680–15688. doi:10.1021/acs.est.0c05624
118. Bartolomei, V.; Sörgel, M.; Gligorovski, S.; Alvarez, E. G.; Gandolfo, A.; Strekowski, R.; Quivet, E.; Held, A.; Zetzsch, C.; Wortham, H. Formation of Indoor Nitrous Acid (HONO) by Light-Induced NO2 Heterogeneous Reactions with White Wall Paint. *Environ. Sci. Pollut. Res.* 2014, *21*, 9259–9269. doi:10.1007/s11356-014-2836-5
119. Wainman, T.; Weschler, C. J.; Lioy, P. J.; Zhang, J. Effects of Surface Type and Relative Humidity on the Production and Concentration of Nitrous Acid in a Model Indoor Environment. *Environ. Sci. Technol.* 2001, *35*, 2200–2206. doi:10.1021/es000879i
120. Jarvis, D. L.; Leaderer, B. P.; Chinn, S.; Burney, P. G. Indoor Nitrous Acid and Respiratory Symptoms and Lung Function in Adults. *Thorax* 2005, *60*, 474–479. doi:10.1136/thx.2004.032177
121. Park, S. S.; Hong, J. H.; Lee, J. H.; Kim, Y. J.; Cho, S. Y.; Kim, S. J. Investigation of Nitrous Acid Concentration in an Indoor Environment Using an in-Situ Monitoring System. *Atmos. Environ.* 2008, *42*, 6586–6596. doi:10.1016/j.atmosenv.2008.05.023
122. Appel, B. R.; Winer, A.; Tokiwa, Y.; Biermann, H. W. Comparison of Atmospheric Nitrous Acid Measurements by Annular Denuder and Differential Optical Absorption Systems. *Atmos. Environ. Part A. Gen. Top* 1990, *24*, 611–616. doi:10.1016/0960-1686(90)90016-G
123. Febo, a.; Perrino, C.; Allegrini, I. Measurement of Nitrous Acid in Milan, Italy, by DOAS and Diffusion Denuders. *Atmos. Environ.* 1996, *30*, 3599–3609. doi:10.1016/1352-2310(96)00069-6

124. Coe, H.; Jones, R. L.; Colin, R.; Carleer, M.; Harrison, R. M.; Peak, J.; Plane, J. M. C.; Smith, N.; Allan, B.; Clemitshaw, K. C.; et al. A Comparison of Differential Optical Absorption Spectrometers for Measurement of NO2, O3, SO2 and HONO. In *EUROTRAC Symposium'96: Transport and Transformation of Pollutants*; Borrell, P. M., Borrell, P., Cvitaš, T., Kelly, K., Seiler, W., Eds.; Computational Mechanics Publications: Southampton, 1997; pp 757–762.
125. Müller, T.; Dubois, R.; Spindler, G.; Brüggemann, E.; Ackermann, R.; Geyer, A.; Platt, U. Measurements of Nitrous Acid by DOAS and Diffusion Denuders: A Comparison. In *Proceedings of EUROTRAC Symposium'98: Transport and Chemical Transformation in the Troposphere, Volume* I; Borrell, P. M., Ed.; WITPress: Southampton, 1999; pp 345–349.
126. Heland, J.; Kleefmann, J.; Kurtenbach, R.; Wiesen, P. A New Instrument to Measure Gaseous Nitrous Acid (HONO) in the Atmosphere. *Environ. Sci. Technol.* 2001, *35*, 3207–3212. doi:10.1021/es000303t
127. Kleffmann, J.; Heland, J.; Kurtenbach, R.; Lörzer, J.; Wiesen, P. A New Instrument (LOPAP) for the Detection of Nitrous Acid (HONO). *Environ. Sci. Pollut. Res* 2002, *9*, 48–54.
128. Gen-fa, Z.; Slanina, S.; Boring, C. B.; Jongejan, P.; Dasgupta, P. Continuous Wet Denuder Measurements of Atmospheric Nitric and Nitrous Acids during the 1999 Atlanta Supersite. *Atmos. Environ.* 2003, *37*, 1351–1364. doi:10.1016/S1352-2310(02)01011-7
129. Takenaka, N.; Terada, H.; Oro, Y.; Hiroi, M.; Yoshikawa, H.; Okitsu, K.; Bandow, H. A New Method for the Measurement of Trace Amounts of HONO in the Atmosphere Using an Air-Dragged Aqua-Membrane-Type Denuder and Fluorescence Detection. *Analyst* 2004, *129*, 1130–1136. doi:10.1039/b407726a
130. Kleffmann, J.; Lörzer, J.; Wiesen, P.; Kern, C.; Trick, S.; Volkamer, R.; Ródenas, M.; Wirtz, K. Intercomparison of the DOAS and LOPAP Techniques for the Detection of Nitrous Acid (HONO). *Atmos. Environ.* 2006, *40*, 3640–3652. doi:10.1016/j.atmosenv.2006.03.027
131. Acker, K.; Febo, A.; Trick, S.; Perrino, C.; Bruno, P.; Wiesen, P.; Möller, D.; Wieprecht, W.; Auel, R.; Giusto, M.; et al. Nitrous Acid in the Urban Area of Rome. *Atmos. Environ.* 2006, *40*, 3123–3133. doi:10.1016/j.atmosenv.2006.01.028
132. Stutz, J.; Oh, H.-J.; Whitlow, S. I.; Anderson, C.; Dibb, J. E.; Flynn, J. H.; Rappenglück, B.; Lefer, B. Simultaneous DOAS and Mist-Chamber IC Measurements of HONO in Houston, TX. *Atmos. Environ.* 2010, *44*, 4090–4098. doi:10.1016/j.atmosenv.2009.02.003
133. Cheng, P.; Cheng, Y.; Lu, K.; Su, H.; Yang, Q.; Zou, Y.; Zhao, Y.; Dong, H.; Zeng, L.; Zhang, Y. An Online Monitoring System for Atmospheric Nitrous Acid (HONO) Based on Stripping Coil and Ion Chromatography. *J. Environ. Sci* 2013, *25*, 895–907. doi:10.1016/S1001-0742(12)60251-4
134. Pinto, J. P.; Dibb, J.; Lee, B. H.; Rappenglück, B.; Wood, E. C.; Levy, M.; Zhang, R.-Y.; Lefer, B.; Ren, X.-R.; Stutz, J.; et al. Intercomparison of Field Measurements of Nitrous Acid (HONO) during the SHARP Campaign. *J. Geophys. Res. Atmos* 2014, *119*, 5583–5601. doi:10.1002/2013JD020287
135. Liu, Y.; Lu, K.; Dong, H.; Li, X.; Cheng, P.; Zou, Q.; Wu, Y.; Liu, X.; Zhang, Y. In Situ Monitoring of Atmospheric Nitrous Acid Based on Multi-Pumping Flow System and Liquid Waveguide Capillary Cell. *J. Environ. Sci. (China)* 2016, *43*, 273–284. doi:10.1016/j.jes.2015.11.034
136. Afif, C.; Jambert, C.; Michoud, V.; Colomb, A.; Eyglunent, G.; Borbon, A.; Daële, V.; Doussin, J.-F.; Perros, P. NitroMAC: An Instrument for the Measurement of HONO and Intercomparison with a Long-Path Absorption Photometer. *J. Environ. Sci. (China)* 2016, *40*, 105–113. doi:10.1016/j.jes.2015.10.024
137. Xue, C.; Ye, C.; Ma, Z.; Liu, P.; Zhang, Y.; Zhang, C.; Tang, K.; Zhang, W.; Zhao, X.; Wang, Y.; et al. Development of Stripping Coil-Ion Chromatograph Method and Intercomparison with CEAS and LOPAP to Measure Atmospheric HONO. *Sci. Total Environ.* 2019, *646*, 187–195. doi:10.1016/j.scitotenv.2018.07.244

138. Xu, Z.; Liu, Y.; Nie, W.; Sun, P.; Chi, X.; Ding, A. Evaluating the Measurement Interference of Wet Rotating-Denuder–Ion Chromatography in Measuring Atmospheric HONO in a Highly Polluted Area. *Atmos. Meas. Tech* 2019, *12*, 6737–6748. doi:10.5194/amt-12-6737-2019
139. Crilley, L. R.; Kramer, L. J.; Ouyang, B.; Duan, J.; Zhang, W.; Tong, S.; Ge, M.; Tang, K.; Qin, M.; Xie, P.; Shaw, M. D.; Lewis, A. C.; Mehra, A.; Bannan, T. J.; Worrall, S. D.; Priestley, M.; Bacak, A.; Coe, H.; Allan, J.; Percival, C. J.; Popoola, O. A. M.; Jones, R. L.; Bloss, W. J. Intercomparison of nitrous acid (HONO) measurement techniques in a megacity (Beijing). *Atmos. Meas. Tech.*, 2019, 12, 6449–6463. doi:10.5194/amt-12-6449-2019.
140. Odabasi, M. Halogenated Volatile Organic Compounds from the Use of Chlorine-Bleach-Containing Household Products. *Environ. Sci. Technol.* 2008, *42*, 1445–1451. doi:10.1021/es702355u
141. Avallone, L. M.; Toohey, D. W. Tests of Halogen Photochemistry Using in Situ Measurements of ClO and BrO in the Lower Polar Stratosphere. *J. Geophys. Res.* 2001, *106*, 10411–10421. doi:10.1029/2000JD900831
142. Harris, G. W.; Klemp, D.; Zenker, T. An Upper Limit on the HCl near-Surface Mixing Ratio over the Atlantic Measured Using TDLAS. *J. Atmos. Chem.* 1992, *15*, 327–332. doi:10.1007/BF00115402
143. Furlani, T. C.; Veres, P. R.; Dawe, K. E. R.; Neuman, J. A.; Brown, S. S.; VandenBoer, T. C.; Young, C. J. Validation of a New Cavity Ring-down Spectrometer for Measuring Tropospheric Gaseous Hydrogen Chloride. *Atmos. Meas. Tech.* 2021, *14*, 5859–5871. doi:10.5194/amt-14-5859-2021
144. Wilkerson, J.; Sayres, D. S.; Smith, J. B.; Allen, N.; Rivero, M.; Greenberg, M.; Martin, T.; Anderson, J. G. In Situ Observations of Stratospheric HCl Using Three-Mirror Integrated Cavity Output Spectroscopy. *Atmos. Meas. Tech.* 2021, *14*, 3597–3613. doi:10.5194/amt-14-3597-2021
145. Keuken, M. P.; Schoonebeek, C. A. M.; van Wensveen-Louter, A.; Slanina, J. Simultaneous Sampling of NH3, HNO3, HC1, SO2 and H2O2 in Ambient Air by a Wet Annular Denuder System. *Atmos. Environ.* 1988, *22*, 2541–2548. doi:10.1016/0004-6981(88)90486-6
146. Lee, B. H.; Lopez-Hilfiker, F. D.; Schroder, J. C.; Campuzano-Jost, P.; Jimenez, J. L.; McDuffie, E. E.; Fibiger, D. L.; Veres, P. R.; Brown, S. S.; Campos, T. L.; et al. Airborne Observations of Reactive Inorganic Chlorine and Bromine Species in the Exhaust of Coal-Fired Power Plants. *J. Geophys. Res. Atmos.* 2018, *123*, 11225–11237. doi:10.1029/2018JD029284
147. Crisp, T. A.; Lerner, B. M.; Williams, E. J.; Quinn, P. K.; Bates, T. S.; Bertram, T. H. Observations of Gas Phase Hydrochloric Acid in the Polluted Marine Boundary Layer. *J. Geophys. Res. Atmos.* 2014, *119*, 6897–6915. doi:10.1002/2013JD020992
148. Kim, S.; Huey, L. G.; Stickel, R. E.; Pierce, R. B.; Chen, G.; Avery, M. A.; Dibb, J. E.; Diskin, G. S.; Sachse, G. W.; McNaughton, C. S.; et al. Airborne Measurements of HCl from the Marine Boundary Layer to Thelower Stratosphere over the North Pacific Ocean during INTEX-B. *Atmos. Chem. Phys. Discuss* 2008, *8*, 3563–3595. doi:10.5194/acpd-8-3563-2008
149. Brown, S. S.; Stutz, J. Nighttime Radical Observations and Chemistry. *Chem. Soc. Rev.* 2012, *41*, 6405–6447. doi:10.1039/c2cs35181a
150. Yokelson, R. J.; Burkholder, J. B.; Fox, R. W.; Talukdar, R. K.; Ravishankara, A. R. Temperature Dependence of the NO3 Absorption Spectrum. *J. Phys. Chem.* 1994, *98*, 13144–13150. doi:10.1021/j100101a009
151. Dubá, W. P.; Brown, S. S.; Osthoff, H. D.; Nunley, M. R.; Ciciora, S. J.; Paris, M. W.; McLaughlin, R. J.; Ravishankara, A. R. Aircraft Instrument for Simultaneous, in Situ Measurement of N O3 and N2 O5 via Pulsed Cavity Ring-down Spectroscopy. *Rev. Sci. Instrum.* 2006, *77*, 034101. doi:10.1063/1.2176058
152. Bitter, M.; Ball, S. M.; Povey, I. M.; Jones, R. L. A Broadband Cavity Ringdown Spectrometer for in-Situ Measurements of Atmospheric Trace Gases. *Atmos. Chem. Phys* 2005, *5*, 2547–2560. doi:10.5194/acp-5-2547-2005

153. Venables, D. S.; Gherman, T.; Orphal, J.; Wenger, J.; Ruth, A. A. High Sensitivity in Situ Monitoring of NO3 in an Atmospheric Simulation Chamber Using Incoherent Broadband Cavity-Enhanced Absorption Spectroscopy. *Environ. Sci. Technol.* 2006, *40*, 6758–6763. doi:10.1021/es061076j
154. Wang, H.; Lu, K. Monitoring Ambient Nitrate Radical by Open-Path Cavity-Enhanced Absorption Spectroscopy. *Anal. Chem.* 2019, *91*, 10687–10693. doi:10.1021/acs.analchem.9b01971
155. Slusher, D. L.; Huey, L. G.; Tanner, D. J.; Flocke, F. M.; Roberts, J. M. A Thermal Dissociation–Chemical Ionization Mass Spectrometry (TD-CIMS) Technique for the Simultaneous Measurement of Peroxyacyl Nitrates and Dinitrogen Pentoxide. *J. Geophys. Res.* 2004, *109*, 1–13. doi:10.1029/2004JD004670
156. Yan, C.; Tham, Y. J.; Zha, Q.; Wang, X.; Xue, L.; Dai, J.; Wang, Z.; Wang, T. Fast Heterogeneous Loss of N2O5 Leads to Significant Nighttime NOx Removal and Nitrate Aerosol Formation at a Coastal Background Environment of Southern China. *Sci. Total Environ.* 2019, *677*, 637–647. doi:10.1016/j.scitotenv.2019.04.389
157. Matsumoto, J.; Kosugi, N.; Imai, H.; Kajii, Y. Development of a Measurement System for Nitrate Radical and Dinitrogen Pentoxide Using a Thermal Conversion/Laser-Induced Fluorescence Technique. *Rev. Sci. Instrum.* 2005, *76*, 3–13. doi:10.1063/1.1927098
158. Wood, E. C.; Wooldridge, P. J.; Freese, J. H.; Albrecht, T.; Cohen, R. C. Prototype for in Situ Detection of Atmospheric NO3 and N2O5 via Laser-Induced Fluorescence. *Environ. Sci. Technol.* 2003, *37*, 5732–5738. doi:10.1021/es034507w
159. Nøjgaard, J. K. Indoor Measurements of the Sum of the Nitrate Radical, NO3, and Nitrogen Pentoxide, N2O5 in Denmark. *Chemosphere* 2010, *79*, 898–904. doi:10.1016/j.chemosphere.2010.02.025
160. King, M. D.; Dick, E. M.; Simpson, W. R. A New Method for the Atmospheric Detection of the Nitrate Radical (NO3). *Atmos. Environ.* 2000, *34*, 685–688. doi:10.1016/S1352-2310(99)00418-5
161. Brown, S. S.; Stark, H.; Ciciora, S. J.; McLaughlin, R. J.; Ravishankara, a R. Simultaneous in Situ Detection of Atmospheric NO3 and N2O5 via Cavity Ring-down Spectroscopy. *Rev. Sci. Instrum.* 2002, *73*, 3291–3301. doi:10.1063/1.1499214
162. Simpson, W. R. Continuous Wave Cavity Ring-down Spectroscopy Applied to in Situ Detection of Dinitrogen Pentoxide (N2O5). *Rev. Sci. Instrum* 2003, *74*, 3442–3452. doi:10.1063/1.1578705
163. Langridge, J. M.; Ball, S. M.; Shillings, A. J. L.; Jones, R. L. A Broadband Absorption Spectrometer Using Light Emitting Diodes for Ultrasensitive, in Situ Trace Gas Detection. *Rev. Sci. Instrum* 2008, *79*, 1–14. 10.1063/1.3046282.
164. Fouqueau, A.; Cirtog, M.; Cazaunau, M.; Pangui, E.; Zapf, P.; Siour, G.; Landsheere, X.; Méjean, G.; Romanini, D.; Picquet-Varrault, B. Implementation of an Incoherent Broadband Cavity-Enhanced Absorption Spectroscopy Technique in an Atmospheric Simulation Chamber for in Situ NO3 Monitoring: Characterization and Validation for Kinetic Studies. *Atmos. Meas. Tech* 2020, *13*, 6311–6323. doi:10.5194/amt-13-6311-2020
165. Li, Z.; Hu, R.; Xie, P.; Hao, C.; Wu, S.; Wang, F.; Wang, Y.; Ling, L.; Liu, J.; Liu, W. Development of a Portable Cavity Ring down Spectroscopy Instrument for Simultaneous, in Situ Measurement of NO3 and N2O5. *Opt. Express* 2018, *26*, A433–7163. doi:10.1364/OE.26.00A433
166. Ventrillard-Courtillot, I.; Sciamma O'Brien, E.; Kassi, S.; Méjean, G.; Romanini, D. Incoherent Broad-Band Cavity-Enhanced Absorption Spectroscopy for Simultaneous Trace Measurements of NO 2 and NO 3 with a LED Source. *Appl. Phys. B* 2010, *101*, 661–669. doi:10.1007/s00340-010-4253-x
167. Kennedy, O. J.; Ouyang, B.; Langridge, J. M.; Daniels, M. J. S.; Bauguitte, S.; Freshwater, R.; Mcleod, M. W.; Ironmonger, C.; Sendall, J.; Norris, O.; et al. An Aircraft Based Three Channel Broadband Cavity Enhanced Absorption Spectrometer for Simultaneous Measurements of NO 3, N 2 O 5 and NO 2. *Atmos. Meas. Tech* 2011, *4*, 1759–1776. doi:10.5194/amt-4-1759-2011

168. Dorn, H. P.; Apodaca, R. L.; Ball, S. M.; Brauers, T.; Brown, S. S.; Crowley, J. N.; Dubé, W. P.; Fuchs, H.; Häseler, R.; Heitmann, U.; et al. Intercomparison of NO3 Radical Detection Instruments in the Atmosphere Simulation Chamber SAPHIR. *Atmos. Meas. Tech* 2013, *6*, 1111–1140. doi:10.5194/amt-6-1111-2013
169. Fuchs, H.; Simpson, W. R.; Apodaca, R. L.; Brauers, T.; Cohen, R. C.; Crowley, J. N.; Dorn, H. P.; Dubé, W. P.; Fry, J. L.; Häseler, R.; et al. Comparison of N2O5 Mixing Ratios during NO3Comp 2007 in SAPHIR. *Atmos. Meas. Tech.* 2012, *5*, 2763–2777. doi:10.5194/amt-5-2763-2012
170. Khan, M. A. H.; Percival, C. J.; Caravan, R. L.; Taatjes, C. A.; Shallcross, D. E. Criegee Intermediates and Their Impacts on the Troposphere. *Environ. Sci. Process Impacts* 2018, *20*, 437–453. doi:10.1039/c7em00585g
171. Novelli, A.; Hens, K.; Tatum Ernest, C.; Martinez, M.; Nölscher, A. C.; Sinha, V.; Paasonen, P.; Petäjä, T.; Sipilä, M.; Elste, T.; et al. Estimating the Atmospheric Concentration of Criegee Intermediates and Their Possible Interference in a FAGE-LIF Instrument. *Atmos. Chem. Phys* 2017, *17*, 7807–7826. doi:10.5194/acp-17-7807-2017
172. Taatjes, C. A. Criegee Intermediates: What Direct Production and Detection Can Teach Us about Reactions of Carbonyl Oxides. *Annu. Rev. Phys. Chem.* 2017, *68*, 183–207. doi:10.1146/annurev-physchem-052516-050739
173. Chhantyal-Pun, R.; Khan, M. A. H.; Taatjes, C. A.; Percival, C. J.; Orr-Ewing, A. J.; Shallcross, D. E. Criegee Intermediates: Production, Detection and Reactivity. *Int. Rev. Phys. Chem.* 2020, *39*, 385–424. doi:10.1080/0144235X.2020.1792104
174. Giorio, C.; Campbell, S. J.; Bruschi, M.; Tampieri, F.; Barbon, A.; Toffoletti, A.; Tapparo, A.; Paijens, C.; Wedlake, A. J.; Grice, P.; et al. Online Quantification of Criegee Intermediates of α-Pinene Ozonolysis by Stabilization with Spin Traps and Proton-Transfer Reaction Mass Spectrometry Detection. *J. Am. Chem. Soc.* 2017, *139*, 3999–4008. doi:10.1021/jacs.6b10981
175. Giorio, C.; Campbell, S. J.; Bruschi, M.; Archibald, A. T.; Kalberer, M. Detection and Identification of Criegee Intermediates from the Ozonolysis of Biogenic and Anthropogenic VOCs: Comparison between Experimental Measurements and Theoretical Calculations. *Faraday Discuss* 2017, *200*, 559–578. doi:10.1039/c7fd00025a
176. Zaytsev, A.; Breitenlechner, M.; Novelli, A.; Fuchs, H.; Knopf, D. A.; Kroll, J. H.; Keutsch, F. N. Application of Chemical Derivatization Techniques Combined with Chemical Ionization Mass Spectrometry to Detect Stabilized Criegee Intermediates and Peroxy Radicals in the Gas Phase. *Atmos. Meas. Tech* 2021, *14*, 2501–2513. doi:10.5194/amt-14-2501-2021
177. Mauldin III, R. L.; Berndt, T.; Sipilä, M.; Paasonen, P.; Petäjä, T.; Kim, S.; Kurtén, T.; Stratmann, F.; Kerminen, V.-M.; Kulmala, M. A New Atmospherically Relevant Oxidant of Sulphur Dioxide. *Nature* 2012, *488*, 193–196. doi:10.1038/nature11278
178. Taatjes, C. A.; Meloni, G.; Selby, T. M.; Trevitt, A. J.; Osborn, D. L.; Percival, C. J.; Shallcross, D. E. Direct Observation of the Gas-Phase Criegee Intermediate (CH2OO). *J. Am. Chem. Soc.* 2008, *130*, 11883–11885. doi:10.1021/ja804165q
179. Welz, O.; Savee, J. D.; Osborn, D. L.; Vasu, S. S.; Percival, C. J.; Shallcross, D. E.; Taatjes, C. a. Direct Kinetic Measurements of Criegee Intermediate (CH2OO) Formed by Reaction of CH2I with O2. *Science* 2012, *335*, 204–207. doi:10.1126/science.1213229
180. Taatjes, C. a.; Welz, O.; Eskola, A. J.; Savee, J. D.; Scheer, A. M.; Shallcross, D. E.; Rotavera, B.; Lee, E. P. F.; Dyke, J. M.; Mok, D. K. W.; et al. Direct Measurements of Conformer-Dependent Reactivity of the Criegee Intermediate CH3CHOO. *Science* 2013, *340*, 177–180. doi:10.1126/science.1234689
181. Chhantyal-Pun, R.; Welz, O.; Savee, J. D.; Eskola, A. J.; Lee, E. P. F.; Blacker, L.; Hill, H. R.; Ashcroft, M.; Khan, M. A. H.; Lloyd-Jones, G. C.; et al. Direct Measurements of Unimolecular and Bimolecular Reaction Kinetics of the Criegee Intermediate (CH3)2COO. *J. Phys. Chem. A.* 2017, *121*, 4–15. doi:10.1021/acs.jpca.6b07810
182. Caravan, R. L.; Vansco, M. F.; Au, K.; Khan, M. A. H.; Li, Y.-L.; Winiberg, F. A. F.; Zuraski, K.; Lin, Y.-H.; Chao, W.; Trongsiriwat, N.; et al. Direct Kinetic Measurements

and Theoretical Predictions of an Isoprene-Derived Criegee Intermediate. *Proc. Natl. Acad. Sci. U S A*. 2020, *117*, 9733–9740. doi:10.1073/pnas.1916711117

183. Sheps, L.; Scully, A. M.; Au, K. UV Absorption Probing of the Conformer-Dependent Reactivity of a Criegee Intermediate CH3CHOO. *Phys. Chem. Chem. Phys.* 2014, *16*, 26701–26706. doi:10.1039/c4cp04408h
184. Lin, H.-Y.; Huang, Y.-H.; Wang, X.; Bowman, J. M.; Nishimura, Y.; Witek, H. A.; Lee, Y.-P. Infrared Identification of the Criegee Intermediates Syn- and anti-CH3CHOO, and Their Distinct Conformation-Dependent Reactivity. *Nat. Commun.* 2015, *6*, 7012. doi:10.1038/ncomms8012.
185. Chung, C.-A.; Lee, Y.-P. Infrared Characterization of Formation and Resonance Stabilization of the Criegee Intermediate Methyl Vinyl Ketone Oxide. *Commun. Chem.* 2021, *4*, 8. doi:10.1038/s42004-020-00447-1
186. Berndt, T.; Herrmann, H.; Kurtén, T. Direct Probing of Criegee Intermediates from Gas-Phase Ozonolysis Using Chemical Ionization Mass Spectrometry. *J. Am. Chem. Soc.* 2017, *139*, 13387–13392. doi:10.1021/jacs.7b05849
187. Bianchi, F.; Kurtén, T.; Riva, M.; Mohr, C.; Rissanen, M. P.; Roldin, P.; Berndt, T.; Crounse, J. D.; Wennberg, P. O.; Mentel, T. F.; et al. Highly Oxygenated Organic Molecules (HOM) from Gas-Phase Autoxidation Involving Peroxy Radicals: A Key Contributor to Atmospheric Aerosol. *Chem. Rev.* 2019, *119*, 3472–3509. doi:10.1021/acs.chemrev.8b00395
188. Emmerson, K. M.; Carslaw, N.; Carslaw, D. C.; Lee, J. D.; McFiggans, G.; Bloss, W. J.; Gravestock, T.; Heard, D. E.; Hopkins, J.; Ingham, T.; et al. Free Radical Modelling Studies during the UK TORCH Campaign in Summer 2003. 2007, Atmos. Chem. Phys, *7*, 167–181. doi:10.5194/acpd-6-10523-2006
189. Chan Miller, C.; Jacob, D. J.; Marais, E. A.; Yu, K.; Travis, K. R.; Kim, P. S.; Fisher, J. A.; Zhu, L.; Wolfe, G. M.; Hanisco, T. F.; et al. Glyoxal Yield from Isoprene Oxidation and Relation to Formaldehyde: Chemical Mechanism, Constraints from SENEX Aircraft Observations, and Interpretation of OMI Satellite Data. *Atmos. Chem. Phys* 2017, *17*, 8725–8738. doi:10.5194/acp-17-8725-2017
190. Volkamer, R.; Platt, U.; Wirtz, K. Primary and Secondary Glyoxal Formation from Aromatics: Experimental Evidence for the Bicycloalkyl – Radical Pathway from Benzene, Toluene, and p-Xylene. *J. Phys. Chem. A* 2001, *105*, 7865–7874. doi:10.1021/jp010152w
191. Gómez Alvarez, E.; Viidanoja, J.; Muñoz, A.; Wirtz, K.; Hjorth, J. Experimental Confirmation of the Dicarbonyl Route in the Photo-Oxidation of Toluene and Benzene. *Environ. Sci. Technol.* 2007, *41*, 8362–8369. doi:10.1021/es0713274
192. Gómez Alvarez, E.; Borrás, E.; Viidanoja, J.; Hjorth, J. Unsaturated Dicarbonyl Products from the OH-Initiated Photo-Oxidation of Furan, 2-Methylfuran and 3-Methylfuran. *Atmos. Environ* 2009, *43*, 1603–1612. doi:10.1016/j.atmosenv.2008.12.019
193. Bierbach, A.; Barnes, I.; Becker, K. H.; Wiesen, E. Atmospheric Chemistry of Unsaturated Carbonyls: Butenedial, 4-Oxo-2-Pentenal, 3-Hexene-2,5-Dione, Maleic Anhydride, 3H-Furan-2-One, and 5-Methyl-3H-Furan-2-One. *Environ. Sci. Technol.* 1994, *28*, 715–729. doi:10.1021/es00053a028
194. Wang, L.; Atkinson, R.; Arey, J. Dicarbonyl Products of the OH Radical-Initiated Reactions of Naphthalene and the Cl- and C2-alkylnaphthalenes. *Environ. Sci. Technol.* 2007, *41*, 2803–2810. doi:10.1021/es0628102
195. Yu, J.; Jeffries, H. E.; Sexton, K. G. Atmospheric Photooxidation of Alkylbenzenes—I. Carbonyl Product Analyses. *Atmos. Environ.* 1997, *31*, 2261–2280. doi:10.1016/S1352-2310(97)00011-3
196. Volkamer, R.; San Martini, F.; Molina, L. T.; Salcedo, D.; Jimenez, J. L.; Molina, M. J. A Missing Sink for Gas-Phase Glyoxal in Mexico City: Formation of Secondary Organic Aerosol. *Geophys. Res. Lett.* 2007, *34*, L19807. doi:10.1029/2007GL030752
197. Fu, T.-M.; Jacob, D. J.; Wittrock, F.; Burrows, J. P.; Vrekoussis, M.; Henze, D. K. Global Budgets of Atmospheric Glyoxal and Methylglyoxal, and Implications for Formation of

Secondary Organic Aerosols. *J. Geophys. Res.* 2008, *113*, D15303. doi:10.1029/2007JD009505
198. Myriokefalitakis, S.; Vrekoussis, M.; Tsigaridis, K.; Wittrock, F.; Richter, A.; Brühl, C.; Volkamer, R.; Burrows, J. P.; Kanakidou, M. The Influence of Natural and Anthropogenic Secondary Sources on the Glyoxal Global Distribution. *Atmos. Chem. Phys.* 2008, *8*, 4965–4981. doi:10.5194/acp-8-4965-2008
199. Stavrakou, T.; Müller, J.-F.; De Smedt, I.; Van Roozendael, M.; Kanakidou, M.; Vrekoussis, M.; Wittrock, F.; Richter, A.; Burrows, J. P. The Continental Source of Glyoxal Estimated by the Synergistic Use of Spaceborne Measurements and Inverse Modelling. *Atmos. Chem. Phys.* 2009, *9*, 8431–8446. doi:10.5194/acp-9-8431-2009
200. Washenfelder, R. A.; Young, C. J.; Brown, S. S.; Angevine, W. M.; Atlas, E. L.; Blake, D. R.; Bon, D. M.; Cubison, M. J.; De Gouw, J. A.; Dusanter, S.; et al. The Glyoxal Budget and Its Contribution to Organic Aerosol for Los Angeles, California, during CalNex 2010. *J. Geophys. Res.* 2011, *116*, 1–17. doi:10.1029/2011JD016314
201. Grosjean, E.; Grosjean, D.; Fraser, M. P.; Cass, G. R. Air Quality Model Evaluation Data for Organics. 2. C1 − C14 Carbonyls in Los Angeles Air. *Environ. Sci. Technol.* 1996, *30*, 2687–2703. doi:10.1021/es950758w
202. Shangari, N.; O'Brien, P. J. The Cytotoxic Mechanism of Glyoxal Involves Oxidative Stress. *Biochem. Pharmacol.* 2004, *68*, 1433–1442. doi:10.1016/j.bcp.2004.06.013
203. Nemet, I.; Varga-Defterdarović, L.; Turk, Z. Methylglyoxal in Food and Living Organisms. *Mol. Nutr. Food Res.* 2006, *50*, 1105–1117. doi:10.1002/mnfr.200600065
204. Lange, J.; Wood, K. D.; Knight, J.; Assimos, D.; Holmes, R. Glyoxal Formation and Its Role in Endogenous Oxalate Synthesis. *Adv. Urol.* 2012, *2012*, 1–5. doi:10.1155/2012/819202
205. Lee, C.; Kim, I.; Lee, J.; Lee, K.-L.; Min, B.; Park, C. Transcriptional Activation of the Aldehyde Reductase YqhD by YqhC and Its Implication in Glyoxal Metabolism of Escherichia Coli K-12. *J. Bacteriol.* 2010, *192*, 4205–4214. doi:10.1128/JB.01127-09
206. Nigro, C.; Leone, A.; Raciti, G. A.; Longo, M.; Mirra, P.; Formisano, P.; Beguinot, F.; Miele, C. Methylglyoxal-Glyoxalase 1 Balance: The Root of Vascular Damage. *IJMS* 2017, *18*, 188. doi:10.3390/ijms18010188
207. Kulkarni, C. A.; Nadtochiy, S. M.; Kennedy, L.; Zhang, J.; Chhim, S.; Alwaseem, H.; Murphy, E.; Fu, D.; Brookes, P. S. ALKBH7 Mediates Necrosis via Rewiring of Glyoxal Metabolism. *Elife* 2020, *9*, e58573. doi:10.7554/eLife.58573
208. Wisthaler, A.; Weschler, C. Reactions of Ozone with Human Skin Lipids: Sources of Carbonyls, Dicarbonyls, and Hydroxycarbonyls in Indoor Air. *Proc. Natl. Acad. Sci. U S A.* 2010, *107*, 6568–6575. doi:10.1073/pnas.0904498106
209. Tuazon, E. C.; Atkinson, R. A Product Study of the Gas-Phase Reaction of Methacrolein with the OH Radical in the Presence of NOx. *Int. J. Chem. Kinet.* 1990, *22*, 591–602. doi:10.1002/kin.550220604
210. Profeta, L. T. M.; Sams, R. L.; Johnson, T. J.; Williams, S. D. Quantitative Infrared Intensity Studies of Vapor-Phase Glyoxal, Methylglyoxal, and 2,3-Butanedione (Diacetyl) with Vibrational Assignments. *J Phys. Chem. A.* 2011, *115*, 9886–9900. doi:10.1021/jp204532x
211. Volkamer, R.; Molina, L. T.; Molina, M. J.; Shirley, T.; Brune, W. H. DOAS Measurement of Glyoxal as an Indicator for Fast VOC Chemistry in Urban Air. *Geophys. Res. Lett* 2005, *32*, 1–4. doi:10.1029/2005GL022616
212. Sinreich, R.; Volkamer, R.; Filsinger, F.; Frieß, U.; Kern, C.; Platt, U.; Sebastián, O.; Wagner, T. MAX-DOAS Detection of Glyoxal during ICARTT 2004. *Atmos. Chem. Phys* 2007, *7*, 1293–1303. doi:10.5194/acp-7-1293-2007
213. Washenfelder, R. a.; Langford, a O.; Fuchs, H.; Brown, S. S. Measurement of Glyoxal Using an Incoherent Broadband Cavity Enhanced Absorption Spectrometer. *Atmos. Chem. Phys. Discuss* 2008, *8*, 16517–16553. doi:10.5194/acpd-8-16517-2008
214. Thalman, R.; Volkamer, R. Inherent Calibration of a Blue LED-CE-DOAS Instrument to Measure Iodine Oxide, Glyoxal, Methyl Glyoxal, Nitrogen Dioxide, Water Vapour and

Aerosol Extinction in Open Cavity Mode. *Atmos. Meas. Tech* 2010, *3*, 1797–1814. doi:10.5194/amt-3-1797-2010

215. Huisman, A. J.; Hottle, J. R.; Coens, K. L.; DiGangi, J. P.; Galloway, M. M.; Kammrath, A.; Keutsch, F. N. Laser-Induced Phosphorescence for the in Situ Detection of Glyoxal at Part per Trillion Mixing Ratios. *Anal. Chem.* 2008, *80*, 5884–5891. doi:10.1021/ac800407b
216. Henry, S. B.; Kammrath, A.; Keutsch, F. N. Quantification of Gas-Phase Glyoxal and Methylglyoxal via the Laser-Induced Phosphorescence of (Methyl)GLyOxal Spectrometry (LIPGLOS) Method. *Atmos. Meas. Tech.* 2012, *5*, 181–192. doi:10.5194/amt-5-181-2012
217. de Gouw, J. A.; de; Goldan, P. D.; Warneke, C.; Kuster, W. C.; Roberts, J. M.; Marchewka, M.; Bertman, S. B.; Pszenny, A. A. P.; Keene, W. C. Validation of Proton Transfer Reaction-Mass Spectrometry (PTR-MS) Measurements of Gas-Phase Organic Compounds in the Atmosphere during the New England Air Quality Study (NEAQS) in 2002. *J. Geophys. Res* 2003, *108*, 4682. doi:10.1029/2003JD003863
218. Michel, E.; Schoon, N.; Amelynck, C.; Guimbaud, C.; Catoire, V.; Arijs, E. A Selected Ion Flow Tube Study of the Reactions of H3O+, NO + and O2+ with Methyl Vinyl Ketone and Some Atmospherically Important Aldehydes. *Int. J. Mass Spectrom.* 2005, *244*, 50–59. doi:10.1016/j.ijms.2005.04.005
219. Guimbaud, C.; Catoire, V.; Bergeat, A.; Michel, E.; Schoon, N.; Amelynck, C.; Labonnette, D.; Poulet, G. Kinetics of the Reactions of Acetone and Glyoxal with O2+ and NO + Ions and Application to the Detection of Oxygenated Volatile Organic Compounds in the Atmosphere by Chemical Ionization Mass Spectrometry. *Int. J. Mass Spectrom* 2007, *263*, 276–288. doi:10.1016/j.ijms.2007.03.006
220. Karl, T.; Guenther, A.; Turnipseed, A.; Tyndall, G.; Artaxo, P.; Martin, S. Rapid Formation of Isoprene Photo-Oxidation Products Observed in Amazonia. *Atmos. Chem. Phys* 2009, *9*, 7753–7767. doi:10.5194/acp-9-7753-2009
221. Ham, J. E.; Wells, J. R. Surface Chemistry of a Pine-Oil Cleaner and Other Terpene Mixtures with Ozone on Vinyl Flooring Tiles. *Chemosphere* 2011, *83*, 327–333. doi:10.1016/j.chemosphere.2010.12.036
222. Wells, J. R.; Morrison, G. C.; Coleman, B. K.; Spicer, C.; Dean, S. W. Kinetics and Reaction Products of Ozone and Surface-Bound Squalene. *J. ASTM Int.* 2008, *5*, 101629. doi:10.1520/JAI101629
223. Jones, B. T.; Ham, J. E. α-Terpineol Reactions with the Nitrate Radical: Rate Constant and Gas-Phase Products. *Atmos. Environ.* 2008, *42*, 6689–6698. doi:10.1016/j.atmosenv.2008.04.017
224. Ham, J. E.; Proper, S. P.; Wells, J. R. Gas-Phase Chemistry of Citronellol with Ozone and OH Radical: Rate Constants and Products. *Atmos. Environ* 2006, *40*, 726–735. doi:10.1016/j.atmosenv.2005.10.004
225. Fick, J.; Nilsson, C.; Andersson, B. Formation of Oxidation Products in a Ventilation System. *Atmos. Environ* 2004, *38*, 5895–5899. doi:10.1016/j.atmosenv.2004.08.020
226. Harrison, J. C.; Wells, J. R. Investigation of Terpinolene + Ozone or Terpinolene + Nitrate Radical Reaction Products Using Denuder/Filter Apparatus. *Atmos. Environ. (1994)* 2013, *80*, 524–532. doi:10.1016/j.atmosenv.2013.08.032
227. Huang, Y.; Ho, S. S. H.; Ho, K. F.; Lee, S. C.; Gao, Y.; Cheng, Y.; Chan, C. S. Characterization of Biogenic Volatile Organic Compounds (BVOCs) in Cleaning Reagents and Air Fresheners in Hong Kong. *Atmos. Environ.* 2011, *45*, 6191–6196. doi:10.1016/j.atmosenv.2011.08.012
228. Ham, J. E.; Jackson, S. R.; Harrison, J. C.; Wells, J. R. Gas-Phase Reaction Products and Yields of Terpinolene with Ozone and Nitric Oxide Using a New Derivatization Agent. *Atmos. Environ.*, 2015, *122*, 513-520. doi:10.1016/j.atmosenv.2015.10.015
229. Stefaniak, A. B.; LeBouf, R. F.; Yi, J.; Ham, J.; Nurkewicz, T.; Schwegler-Berry, D. E.; Chen, B. T.; Wells, J. R.; Duling, M. G.; Lawrence, R. B.; et al. Characterization of Chemical Contaminants Generated by a Desktop Fused Deposition Modeling 3-Dimensional Printer Characterization of Chemical Contaminants Generated by a Desktop

Fused Deposition Modeling 3. *J. Occup. Environ. Hyg.* 2017, *14*, 540–550. doi:10.1080/15459624.2017.1302589

230. Forester, C. D.; Ham, J. E.; Wells, J. R. Geraniol (2,6-Dimethyl-2,6-Octadien-8-Ol) Reactions with Ozone and OH Radical: Rate Constants and Gas-Phase Products. *Atmos. Environ* 2007, *41*, 1188–1199. doi:10.1016/j.atmosenv.2006.09.042
231. Forester, C. D.; Wells, J. R. Yields of Carbonyl Products from Gas-Phase Reactions of Fragrance Compounds with OH Radical and Ozone. *Environ. Sci. Technol.* 2009, *43*, 3561–3568. doi:10.1021/es803465v
232. Forester, C. D.; Ham, J. E.; Wells, J. R. β-Ionone Reactions with Ozone and OH Radical: Rate Constants and Gas-Phase Products. *Atmos. Environ.* 2007, *41*, 8758–8771. doi:10.1016/j.atmosenv.2007.07.047
233. Szulejko, J.; Kim, K.-H. Derivatization Techniques for Determination of Carbonyls in Air. *Trends Anal. Chem.* 2015, *64*, 29–41. doi:10.1016/j.trac.2014.08.010
234. Jackson, S. R.; Ham, J. E.; Harrison, J. C.; Wells, J. R. Identification and Quantification of Carbonyl-Containing α-Pinene Ozonolysis Products Using O-Tert-Butylhydroxylamine Hydrochloride. *J. Atmos Chem.* 2017, *74*, 325–338. doi:10.1007/s10874-016-9344-6
235. Zhang, J.; Zhang, L.; Fan, Z.; Ilacqua, V. Development of the Personal Aldehydes and Ketones Sampler Based upon DNSH Derivatization on Solid Sorbent. *Environ. Sci. Technol.* 2000, *34*, 2601–2607. doi:10.1021/es9911869
236. Fujioka, K.; Shibamoto, T. Determination of Toxic Carbonyl Compounds in Cigarette Smoke. *Environ. Toxicol.* 2006, *21*, 47–54. doi:10.1002/tox.20153
237. Farmer, D. K.; Vance, M. E.; Abbatt, J. P. D.; Abeleira, A.; Alves, M. R.; Arata, C.; Boedicker, E.; Bourne, S.; Cardoso-Saldaña, F.; Corsi, R.; et al. Overview of HOMEChem: House Observations of Microbial and Environmental Chemistry. *Environ. Sci. Process Impacts* 2019, *21*, 1280–1300. doi:10.1039/c9em00228f
238. Thalman, R.; Baeza-Romero, M. T.; Ball, S. M.; Daniels, M. J. S.; Goodall, I. C. A.; Henry, S. B.; Karl, T.; Keutsch, F. N.; Kim, S.; Mak, J.; et al. Instrument Intercomparison of Glyoxal, Methyl Glyoxal and NO 2. *Atmos. Meas. Tech* 2015, *8*, 1835–1862. doi:10.5194/amt-8-1835-2015
239. Michoud, V.; Sauvage, S.; Léonardis, T.; Fronval, I.; Kukui, A.; Locoge, N.; Dusanter, S. Field Measurements of Methylglyoxal Using Proton Transfer Reaction Time-of-Flight Mass Spectrometry and Comparison to the DNPH–HPLC–UV Method. *Atmos. Meas. Tech* 2018, *11*, 5729–5740. doi:10.5194/amt-11-5729-2018
240. Hofzumahaus, A. Measurement of Photolysis Frequencies in the Atmosphere. In *Analytical Techniques for Atmospheric Measurement*; Heard, D. E., Ed.; Blackwell: Oxford, 2006.
241. Bohn, B.; Heard, D. E.; Mihalopoulos, N.; Plass-Dülmer, C.; Schmitt, R.; Whalley, L. K. Characterisation and Improvement of j(O1D) Filter Radiometers. *Atmos. Meas. Tech.* 2016, *9*, 3455–3466. doi:10.5194/amt-9-3455-2016
242. Kowal, S. F.; Allen, S. R.; Kahan, T. F. Wavelength-Resolved Photon Fluxes of Indoor Light Sources: Implications for HOx Production. *Environ. Sci. Technol.* 2017, *51*, 10423–10430. doi:10.1021/acs.est.7b02015
243. Blocquet, M.; Guo, F.; Mendez, M.; Ward, M.; Coudert, S.; Batut, S.; Hecquet, C.; Blond, N.; Fittschen, C.; Schoemaecker, C. Impact of the Spectral and Spatial Properties of Natural Light on Indoor Gas-Phase Chemistry: Experimental and Modeling Study. *Indoor Air* 2018, *28*, 426–440. doi:10.1111/ina.12450
244. Kleffmann, J. Comment on "Wavelength-Resolved Photon Fluxes of Indoor Light Sources: Implications for HO x Production". *Environ. Sci. Technol.* 2018, *52*, 11964–11965. doi:10.1021/acs.est.8b03960